

1 **Quantifying the response of water and carbon balances to land**
2 **cover and climate extremes across Germany.**

3 Karim Pyarali^{1,2*}, Lulu Zhang^{2*}, Ning Liu⁴, Abdulhakeem Al-Qubati^{1,2} and Ge Sun^{3*}

4 ¹Technische Universität Dresden, Helmholtzstr. 10, 01069, Dresden, Germany.

5 ²United Nations University, Institute for Integrated Management of Material Fluxes and of Resources, Ammonstrasse
6 74, 01067, Dresden, Germany.

7 ³Eastern Forest Environmental Threat Assessment Center, Southern Research Station, USDA Forest Service, Research
8 Triangle Park, NC 27713, USA.

9 ⁴CSIRO Environment, Canberra ACT 2601.

10 *Corresponding authors: Karim Pyarali (karim.pyarali@tu-dresden.de); Lulu Zhang (lzhang@unu.edu); Ge Sun
11 (Ge.Sun@usda.gov)

12

Formatted: German (Germany)

Abstract. Land cover and extreme weather events are closely connected to ecosystem services like water yield and carbon sequestration. Understanding how carbon and water respond to human disturbances is critical for managing these resources and realize desired ecosystem services at the national level. The monthly scale ecosystem model, Water Supply Stress Index (WaSSI), was tested and applied across Germany for mapping carbon and water balances from 2001 to 2019. We estimated that ecosystems in Germany generate 84.86 billion m³ of water yield, and sequester 106.03 Tg of carbon annually on average. Most of the precipitation was lost as evapotranspiration in eastern states that were comparatively drier in river flows than the rest of the country. Croplands, urban areas and Evergreen Needle Forests (ENF) provide 82.5% of the national water yield, while the forest lands share the majority (56.3%) of land carbon sequestration, altogether. Our simulation results highlight the importance of sparse land covers (e.g. wetlands) in carbon sequestration. Findings also suggest that national water yield and carbon balances are sensitive to extreme events such as the floods in 2002 and 2013 and the extreme drought in 2003 and 2018. We found that hydrologic buffers from the previous year played an important role in mitigating negative impacts on both carbon and water availability. This study highlights that, when integrated with local data, a relatively simple modelling approach is adequate to quantify the coupled water and carbon responses to climatic and land cover variability at a large scale. We conclude that land management of both forests and croplands is vital to sustain ecosystem services under a changing climate at regional to national levels.

1. Introduction

Ecosystem services such as water yield and carbon sequestration are intimately linked with land cover and climate extremes. The two key ecosystem services support life and economic activity (Morales et al., 2005). The tightly coupled links between water and carbon cycles through parameters such as precipitation, temperature, evapotranspiration (ET), and ecosystem services are well recognized (Beer et al., 2007; Sun et al., 2011). However, it is still unclear how changes in land cover and climate extremes have impacted these services in Germany at a national level. These services are challenging to measure directly, but an ecosystem services model can be applied to estimate them across the German landscape at a sub-basin scale.

Changes in land cover are driven by multiple interconnected reasons, two of them are improving living standards and population growth (Allan et al., 2022). Studies have shown that land cover change greatly reduces ecosystem services, but the impact varies spatially and temporally (Hasan et al., 2020). According to Pandey & Ghosh (2023), and Salerno et al. (2018), urbanization disrupts regulating service for e.g., water purification, soil retention, and climate regulation. On the other hand, Arowolo et al. (2018), and Cui et al. (2021), observed that expansion of cropland often increases goods from provisioning services such as food, fodder and water yield. A recent survey in 2022 from the German national forest inventory found that since 2017, the German forest has become a source of carbon dioxide, instead of being a sink. The reason behind the change in ecosystem functions is the high loss of living biomass due to climate change and low forest growth (Fourth Federal Forest Inventory 2022, 2024).

Another environmental phenomena that impact ecosystem services are extreme climate events (e.g. droughts & extreme precipitation). Catastrophic weather events not only made countries in the Global South but also in Global North vulnerable. Germany's 2021 summer flood resulted in a loss of 220 lives and US\$ 40 Billion (Schumacher, 2022); the incurred damages from the 2003 drought, primarily on agriculture, were approximately US\$13 Billion across Europe (Eisenreich, 2005). Germany has seen an increase in the intensity and frequency of heavy rainfall, more in winter than in summer. The air temperatures are also projected to rise by 1.6 to 3.8°C by 2080 (Schröter et al., 2005). A shift in precipitation season has been observed, which will potentially increase the risks of floods during winter and decrease the water supply during summer periods (Schröter et al., 2005). The extreme events are changing due to climate change. Their impacts may reduce terrestrial carbon uptake or gross primary productivity (GPP) (Williams et al., 2014), which negatively affects other factors within the co-evolved processes of carbon-water cycle in an integrated terrestrial system (Zhang et al., 2018). Potentially leading to adverse effects on regional food and livelihood security.

Although ecosystem services are essential and well-recognized in Germany, national-scale studies on both carbon and water yield are still lacking. There are multiple studies that focus on a specific land cover type or specific ecosystem services at the European, national or subnational scales. For example, Potter & Pass (2024), estimated the changes in

Deleted: the tradeoffs between...how carbon and water and how they...respond to human disturbances is critical for managing these resources and realize desired ecosystem services at the national level quantifying these

Deleted: ecosystem

Deleted: services... The monthly scale ecosystem model, Water Supply Stress Index (WaSSI) model

Deleted: -

Deleted: s

Deleted: m...³

Deleted: discharge...and sequesters...106.03 Tg of carbon annually on average. The ...ost of the precipitation was lost as evapotranspiration in eastern states that were comparatively drier in river flows than the rest of the country,...as most of their precipitation was lost as evapotranspiration. ...croplands, urban areas and Evergreen Needle Forests (ENF) provide 82.5% of the national water yield, while the forest lands share sequester...the majority (56.3%) share...of land carbon sequestration (56.3%) altogether. Our The...simulation results highlight the importance of sparse land covers (e.g. wetlands) in carbon sequestration. Findings also suggest that national water yield and carbon balances are sensitive to extreme events such as the floods . I...in 2002 and 2013 and , due to high precipitation, the stocks of key ecosystem services were notably higher. Similarly, during ...he extreme drought years in 2003 and 2018. . the services were reduced drastically, but...Ww... found that hydrologic buffers from the previous year played an important role in mitigating negative impacts on both carbon and water availability. This study highlights that, when integrated with local data, a relatively simple modelling approach is adequate to quantify answer questions of ...he coupled water and carbon responses to climatic and

Deleted: ...impacted

Deleted: Pandey & Ghosh (2023),

Formatted: Font: 10 pt, Font color: Black

Deleted: Salerno et al. (2018)

Deleted: Arowolo et al. (2018)

Deleted: Cui et al. (2021)

Deleted: (Fourth Federal Forest Inventory 2022, 2024)

Deleted: floods

Deleted: (Schumacher, 2022)

Deleted: (Eisenreich, 2005)... Germany has seen an increase in the intensity and frequency of heavy rainfall, m

Deleted: (Schröter et al., 2005)

Deleted: (Schröter et al., 2005)

Deleted: (Williams et al., 2014)... , w. W

Deleted: (Zhang et al., 2018)

Deleted: Potter & Pass (2024)

Formatted: Font: 10 pt, Font color: Black

183 net primary productivity (NEP or carbon sequestration) for Western Europe, including Germany. [Gutsch et al. \(2018\)](#),
184 assessed German forest ecosystem services under climate change and different management scenarios. Their results
185 showed that climate change has negative impacts on water percolation and positive impacts on carbon sequestration.
186 Using agricultural long-term field experiments, carbon sequestration was projected to increase in the southern parts
187 of Germany, indicating higher productivity, and decrease in central and east Germany where poor soil will further
188 reduce the productivity ([Donmez et al., 2024](#)). Other studies used regional analysis to assess water or carbon cycles
189 ([Al-Qubati et al., 2023](#); [Prescher et al., 2010](#); [Ungaro et al., 2021](#); [Wu et al., 2021](#)). The lack of integrated water-
190 carbon cycles assessment hampers deriving national or regional adaptive land management strategies to alleviate the
191 adverse impacts resulting from environmental and climate change, particularly in the long term.

Deleted: Gutsch et al. (2018)

192 Furthermore, we observed a varied response of the coupled water-carbon cycle to changes in land cover and climate
193 ([Cheng et al., 2017](#); [Jung et al., 2017](#); [Zeng et al., 2018](#)). The variation is manifested by the coupled mechanisms
194 occurring at multiple timescales. These may be short-term leaf-gas exchanges, monthly or annual ET and carbon
195 accumulation, and long-term water yield and species composition. This *emphasises* that a single type of observation
196 is not sufficient to provide the robust validation needed to address the response of water and carbon cycles to
197 environmental disturbances or climate shocks ([Margulis et al., 2006](#)). [Gentine et al. \(2019\)](#), argued that terrestrial
198 water-carbon cycles must be investigated as an integrated system. They recognized the importance of incorporating
199 multiple observations on different timescales from various sources to better validate model simulations, which may
200 reduce uncertainties, mitigate bias, and provide better predictions. Unfortunately, the suggested approach is seldomly
201 applied in hydrological modelling (e.g. [G. Sun et al., 2011, 2023](#); [J. Zhang et al., 2022](#); [Y. Zhang et al., 2016](#)). Thus,
202 impeding the improvement of our predictive ability to quantify the potential water-carbon changes and consequences
203 that are vital to effective policy decision-making for developing climate adaptation and mitigation strategies.
204 Therefore, we integrated multi-timescale observations and information sources in our model to validate simulated
205 water yield and carbon sequestration. We used gauged river discharge (Q), in-situ measured ET and GPP from eddy
206 flux towers, and remotely sensed ET and GPP data for model validation.

Deleted: (Cheng et al., 2017; Jung et al., 2017; Zeng et al., 2018)...

Deleted: (Margulis et al., 2006)

Deleted: Gentine et al. (2019)

Deleted: (e.g. G. Sun et al., 2011, 2023; J. Zhang et al., 2022; Y. Zhang et al., 2016)

207 In this study, WaSSI, an ecosystem service model, was applied on a monthly *and subbasin (804)* resolution to simulate
208 the water and carbon *processes* across the different land covers within Germany ([Sun et al., 2011](#)). The model has
209 been used globally for various purposes and under different climatic and socioeconomic conditions ([Averyt et al.,](#)
210 [2011](#); [Caldwell et al., 2011, 2014, 2012](#); [N. Liu et al., 2020](#); [G. Sun et al., 2011](#); [S. Sun et al., 2015](#); [McNulty et al.,](#)
211 [2016](#)), in countries like the United States of America, Rwanda, Australia, *Turkiye, Nepal* and China ([Chen et al., 2024](#);
212 [Jin et al., 2025](#); [Liu, 2017](#); [Liu et al., 2013](#); [McNulty et al., 2016](#); [Sun et al., 2011](#)). By validating the WaSSI model,
213 we aim to have an improved understanding of the response of water-carbon cycles on German land cover with climate
214 variability at a watershed scale. Furthermore, we focus on three questions: (i) How did ET, water yield and NEP vary
215 over time and space? (ii) *How did* different land cover contribute to water yield and carbon sequestration? and (iii) to
216 what extent and how sensitive are the two ecosystem services to extreme weather events?

Deleted: the Water Supply Stress Index (

Deleted:)

Deleted: process

Deleted: (Sun et al., 2011)

Deleted: (Averyt et al., 2011; Caldwell et al., 2011, 2014, 2012; N. Liu et al., 2020; G. Sun et al., 2011; S. Sun et al., 2015; McNulty et al., 2016;)

Deleted: how

Deleted: (i.e., droughts and floods)

217 2. Methodology and Data

218 The WaSSI model merges the water and carbon cycle using water use efficiency (WUE) parameters estimated from
219 global eddy flux observations. It is made up of two components: a hydrological and a carbon sub-model. The required
220 inputs are precipitation, temperature, digital elevation model, land cover, fractional impervious cover, leaf area index
221 (LAI), and soil parameters, while the outputs are Q, ET, GPP, and net ecosystem exchange (NEE) ([Liu, 2017](#)).
222 Transboundary inflows and outflows were not accounted in this study; therefore, watersheds close to Germany's
223 boundary, which accumulated their flow across the border, were not considered.

Deleted: (Liu, 2017)

Deleted: ,

224 The WaSSI model estimates *land cover-specific* water yield (mm per month), which can be aggregated as flow volume
225 *downstream* (m³ per month) for any individual watersheds. The hydrologic fluxes estimated are snow melt, snow
226 accumulation, soil storage, surface flow, base flow, routed flow accumulation, and ET ([Sun et al., 2011](#)). The model
227 employs a conceptual method ([McCabe & Wolock, 1999](#)), that uses the monthly average temperature and mean average
228 elevation of a watershed to partition precipitation into rainfall and snowfall, estimate the rate of snow melt, and
229 calculate the mean monthly snow water equivalent for each watershed ([Caldwell et al., 2012](#)). The Sacramento Soil
230 Moisture Accounting (SAC-SMA) model was used for soil and runoff parameters, which runs infiltration, baseflow,

Deleted: cover specific

Deleted: down streams

Deleted: (Sun et al., 2011)

Deleted: (McCabe & Wolock, 1999)

Formatted: Font: 10 pt, Font color: Black

Deleted: (Caldwell et al., 2012)

257 surface runoff, and soil moisture processes, while also constraints ET estimates based on soil water content. For ET
 258 estimations, we used the Type II regression model from (Fang et al., 2015), where the ET model was developed using
 259 quality-controlled global data from more than 200 eddy flux sites (Pastorello et al., 2020), incorporating the three most
 260 commonly available biophysical parameters precipitation (P), potential ET (PET) (Temperature based) and LAI in the
 261 following equation:

$$ET = -4.79 + 0.75PET + 3.92LAI + 0.04P \quad (1)$$

262 WaSSI estimates three main components of the carbon cycles: (i) GPP or total carbon uptake, (ii) ecosystem
 263 respiration (Re) representing carbon loss, and (iii) Net Ecosystem Productivity (NEP) or negative Net Ecosystem
 264 Exchange (NEE) or carbon sequestration.

$$NEP = -NEE = -(Re - GPP) \quad (2)$$

265 Furthermore, a closely coupled relationship between ET and GPP has been found in multiple studies (Law et al., 2002;
 266 Sun et al., 2011), as presented in Equation 3. In the WaSSI model, according to G. Sun et al., (2011), the relationship
 267 of monthly GPP with ET was estimated using linear regression for each land cover. Furthermore, land cover-specific
 268 WUE parameters were used, which were estimated using 142 eddy flux tower data (Zhang et al., 2016). Similarly, the
 269 Re from heterotrophic and autotrophic bacteria can be estimated using Equation 4, where regression coefficients are
 270 estimated from eddy flux data. The coefficient (a, m, and n) values used in this study are provided in Table S1.

$$GPP = a \times ET \quad (3)$$

$$Re = m + n \times GPP \quad (4)$$

271 2.1. Model Validation

272 We validated the model outputs using both in-situ observed data (e.g., stream discharge data from gauge stations and
 273 ET eddy flux data) and remotely sensed data (e.g., ET and GPP estimates from satellites). The temporal resolution of
 274 the WaSSI model output was monthly. The discharge was validated for twelve upstream watersheds across Germany
 275 (Fig. 1). The chosen upstream stations were selected to ensure spatial coverage across Germany, representing the
 276 country's major climatic zones, land use, and land cover types. Stations with long and continuous discharge records
 277 were prioritised. The performance criteria to determine the accuracy of outputs are model bias (%), coefficient of
 278 determination (R^2), scatter plots, Nash-Sutcliffe efficiency (NSE), and Kling-Gupta efficiency (KGE). The estimated
 279 ET was validated against data on different timescales. Simulated ET was compared with daily data from multiple eddy
 280 flux towers, monthly ET from Moderate Resolution Imaging Spectroradiometer (MODIS) (MOD16A2GF) (Running
 281 et al., 2019b), and watershed-specific water balance values, which were calculated by subtracting discharge from
 282 precipitation, on a monthly and annual timescale. Depending on the validation datasets, values were summed to either
 283 monthly or annual timesteps. For carbon, we compared the GPP estimates with GPP measurements from eddy flux
 284 towers, MODIS GPP (MOD17A2HGF) and Copernicus Global Land Service (CGLS) GPP (Running et al., 2019a;
 285 Smets et al., 2019). A monthly land cover-specific validation was conducted between modelled GPP and observed
 286 GPP. Where observed GPP estimates were developed using the daytime partitioning method (GPP_DT_VUT_REF).
 287 Further details for each validation dataset are provided in the following section 2.3. Since the observed data from the
 288 gauge stations and eddy flux towers did not overlap, therefore, joint evaluation at the same subbasin for both Q and
 289 ET was not possible in this study.

Deleted: (Fang et al., 2015)

Deleted: (Pastorello et al., 2020)

Deleted: . Equation 2 estimates the amount of NEP by subtracting Re from GPP.

Deleted: (Law et al., 2002; Sun et al., 2011)

Deleted: (2011)

Deleted: GPP is linearly correlated to ET and

Deleted: specific

Deleted: (Zhang et al., 2016)

Deleted: in the supporting documents

Deleted: Initially, the

Deleted: ,

Deleted:

Deleted: monthly

Deleted: ,

Deleted: several

Deleted: data, including d

Deleted: MODIS

Deleted: ET

Deleted: (Running et al., 2019b)

Deleted: Q

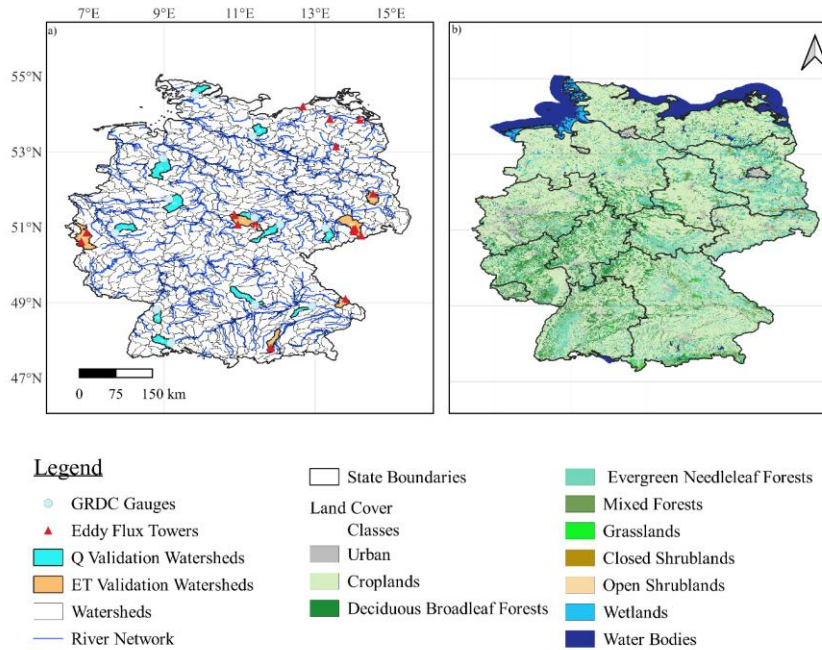
Deleted:

Deleted: MODIS

Deleted: (Running et al., 2019a; Smets et al., 2019)

Deleted: , and CGLS GPP

Deleted:



316

317 **Figure 1:** A map of the study area presenting a) Germany's boundaries with all the 804 watersheds delineated, Global
 318 Runoff Data Center's (GRDC) gauge station locations, major rivers, eddy flux tower sites and representative
 319 watersheds for [streamflow \(Q\)](#) and [evapotranspiration \(ET\)](#) validation and b) Germany's land cover and state
 320 boundaries.

321 **2.2. Input Data**

322 **2.2.1. Study Area**

323 [Germany](#), with an area of 357,168 km², consists of sixteen states. Approximately 83.5 million people reside across
 324 five major river basins that fall within Germany (Rhine, Danube, Elbe, Weser, and Ems). Due to cross-boundary flows,
 325 Germany has bilateral water treaties with all of its neighbours. The climatic conditions span from maritime to
 326 continental. The annual mean temperature ranges from 9 to 11°C, and the annual precipitation ranges from 450 mm
 327 to 970 mm (Kosanic et al., 2019). The land use is dominated by agriculture (61%) and forests (29%). Furthermore,
 328 the built-up area (6%) is continuously expanding as cities grow due to urbanization. Socio-economically there is a
 329 clear divide between the Eastern and Western states due to the Soviet-era policies. In this study, Germany was
 330 delineated into 804 subbasins as the modeling units using a high-resolution digital elevation model (Fig. 1).

331 **2.2.2. Climate Data**

332 Climate data (i.e., precipitation and temperature) is sourced from Germany's national meteorological service ([DWD](#),
 333 2018). Datasets have a spatial resolution of 1km and a temporal resolution of months. The gridded data are prepared
 334 by estimating monthly deviations for each station, which are then interpolated using inverse squared distance weighted
 335 interpolation and transformed back into real values using reference grids (Kaspar et al., 2013).

Formatted: Not Highlight

Formatted: Font: 10 pt, Not Bold

Deleted: as shown in Fig. 1,

Deleted: (DWD, 2018)

Deleted: (Kaspar et al., 2013)

339 **2.2.3. Land cover classification**

340 CORINE land cover (CLC) map of 2018 with a 100 m spatial resolution was used in this study (EEA, 2021). Validation
 341 studies showed that it can capture land cover with an accuracy of 85% (Büttner et al., 2021; Keil, 2017). This study
 342 reclassified land cover into 10 major classes. Table S2 shows the range of CLC classes that were merged along with
 343 their percentage across Germany. The selection of 10 classes was based on the availability of water-use efficiency
 344 (WUE) parameters. These 10 classes encompass all dominant ecosystem types across the study.

- Deleted:
- Deleted: (EEA, 2021)
- Deleted: (Büttner et al., 2021; Keil, 2017)
- Deleted: to reduce complexity

345 **2.2.4. Leaf Area Index**

346 Climate Data Record's (CDR) Vegetation (VGT) sensor LAI was used. The data is available from 2001 to 2014, with
 347 a 10-day temporal and 1km spatial resolution. All pixels with an invalid LAI status were removed during quality
 348 control. Invalid LAI status refers to pixel values that do not fall within an expected range (Verger et al., 2018).
 349 Validation studies of this product showed that it underestimates ground data with a bias of 0.31 and a correlation of
 350 0.72, while against multiple satellite datasets, it overestimates with biases ranging between 0.03 (for MODIS) to 0.36
 351 (for GLOBCARBON) (Camacho & Cernicharo, 2014).

- Deleted: (Verger et al., 2018)
- Deleted: (Camacho & Cernicharo, 2014)
- Formatted: Font: 10 pt, Font color: Black

352 **2.2.5. Fractional impervious cover and soil data**

353 The fractional impervious cover is derived from the Global Man-made Impervious Surface (GMIS) dataset (Brown
 354 de Colstoun et al., 2017). It has a spatial resolution of 30m.

- Deleted: (Brown de Colstoun et al., 2017)

355 Digital soil map BUEK 200 was used to estimate eleven soil parameters following Y. Zhang et al. (2011) and Anderson
 356 et al. (2006). Land cover and soil properties were used to obtain the curve number (CN) that controls the partitioning
 357 of soil into upper and lower zones. The water allocation between tenses and free water storage is determined by soil
 358 composition. The final product has a spatial resolution of 500 m.

- Deleted: Y. Zhang et al. (2011)
- Deleted: Anderson et al. (2006)

359 **2.3. Validation Data**

360 **2.3.1. Stream Discharge Data**

361 The discharge data used for validation are sourced from the Global Runoff Data Center (GRDC). Twelve upstream
 362 stations were identified from a large group of stations for validation of discharge in this work. The selection focused
 363 on upstream watersheds that have less anthropogenic influence (e.g. dams), thus representing natural processes
 364 reasonably well. Furthermore, these stations had continuous long-term discharge data, they represent different climatic
 365 zones in Germany, and they capture diverse land use and land cover types. The location of stations can be observed
 366 in Fig. 1, while their names and ID are provided in Table S3.

- Deleted: because
- Deleted: influences
- Deleted: The
- Deleted: were selected for different regions of Germany to ensure different land uses and land covers were validated.

367 **2.3.2. Eddy Flux ET and GPP**

368 ET and GPP in-situ measurements were acquired from the FLUXNET2015 database (Pastorello et al., 2020). The data
 369 available is quality-controlled. The gaps within the data are filled and corrected following standardised
 370 FLUXNET2015 procedures, which apply algorithms to ensure temporal continuity and consistent flux measurements.
 371 Furthermore, the energy balance closure correction factors (EBC_CF) were used to correct these datasets. The
 372 EBC_CF were estimated using three different methods each assuming that the Bowen ratio holds true. In this study,
 373 monthly latent heat turbulent flux (LE) was converted to ET with and without energy closure corrections and GPP
 374 was calculated using the daytime partitioning method (Pastorello et al., 2020).

- Deleted: (Pastorello et al., 2020)
- Deleted: quality controlled
- Deleted: and
- Deleted: t
- Deleted: to offer high-quality information.
- Deleted: E

375 **2.3.3. MODIS ET and GPP Data**

376 The MODIS ET product MOD16A2GF is employed in this work (Running et al., 2019b). The remote sensing data is
 377 used to compare the spatial variation of model output. MODIS has a spatial resolution of 500m and a temporal
 378 resolution of 8-day. The ET estimation follows the Penman-Monteith equation (Running et al., 2019b). The product
 379 has been comprehensively validated in multiple studies (Kim et al., 2012; Liu et al., 2015; Trambauer et al., 2014;
 380 Velpuri et al., 2013) and used to evaluate the output of hydrological models (Sun et al., 2011). This study used a
 381 monthly sum of ET values and spatial average calculated on a sub-watershed scale.

- Deleted: (Pastorello et al., 2020)
- Deleted: Moderate Resolution Imaging Spectroradiometer (
- Deleted:)
- Deleted: (Running et al., 2019b)
- Deleted: (Running et al., 2019b)
- Deleted: (Kim et al., 2012; Liu et al., 2015; Trambauer et al., 2014; Velpuri et al., 2013)
- Deleted: (Sun et al., 2011)

410 The gap-filled GPP product employed in this study is MOD17A2HGF, with a spatial resolution of 500m and a
411 temporal resolution of 8-day (Running et al., 2019a). It follows Monteith's logic and uses land cover specific light
412 use efficiency (ϵ), fraction of absorbed photosynthetically active radiation (FPAR), incident photosynthetically active
413 radiation (IPAR), the deficit of vapor pressure, and minimum air temperature (Running et al., 2019a). Insights on the
414 application and validation of MODIS-GPP are provided in multiple studies (Liu et al., 2015; Sun et al., 2011; Turner
415 et al., 2006; Wang et al., 2017; Zhu et al., 2018).

416 CGLS GPP are derived from the Gross Dry Matter Productivity (GDMP) values (Smets et al., 2019). We used the
417 version 2 product from SPOT/VGT and PROBA-V satellites to evaluate the model GPP estimates for the period of
418 2001 – 2019. The GDMP product has a spatial and temporal resolution of 1-km and 10-day. It represents the additional
419 gross dry biomass stored in vegetation, which could be converted into gross carbon uptake by multiplying it with a
420 scaling factor of 0.45 gC/gDM (Smets et al., 2019).

$$GPP (gC m^{-2} day^{-1}) = GDMP (kg DM ha^{-1} day^{-1}) * 0.45 * 0.1 \quad (5)$$

421 3. Results

422 3.1. Model Validation

423 3.1.1. Discharge Validation

424 The hydrograph plots reveal that the model, in general, is able to simulate the monthly flows reasonably well (Fig. 2).
425 Furthermore, the model discharge validated on a monthly scale gives KGE for eight out of the twelve watersheds
426 above 0.5 and NSE for six out of twelve watersheds greater than 0.6, as shown in Table S3. While on an annual scale
427 the values of model bias (%) for eleven out of the twelve stations are between -25% to 25% and for R² ten out of
428 twelve stations are above 0.60, as presented in Table S4. The scatter plot between modelled and observed discharge,
429 across the twelve watersheds on both annual and monthly scales, is presented in Fig. S1. The plot shows high
430 correlation between the two datasets suggesting the model performs reasonably well. Except for the Wasserthaleben
431 station, where the model performance is weak with bias equal to 131.8 % and annual R² of 0.18.

Deleted: (Running et al., 2019a)

Deleted: (Running et al., 2019a)

Deleted: (Liu et al., 2015; Sun et al., 2011; Turner et al., 2006; Wang et al., 2017; Zhu et al., 2018)

Deleted: Copernicus Global Land Service (

Deleted:)

Deleted: (Smets et al., 2019)

Deleted: , as shown in the following equation

Deleted: (Smets et al., 2019):

Deleted: , as shown in

Deleted: M

Deleted: Kling-Gupta efficiency (

Deleted:)

Deleted: were

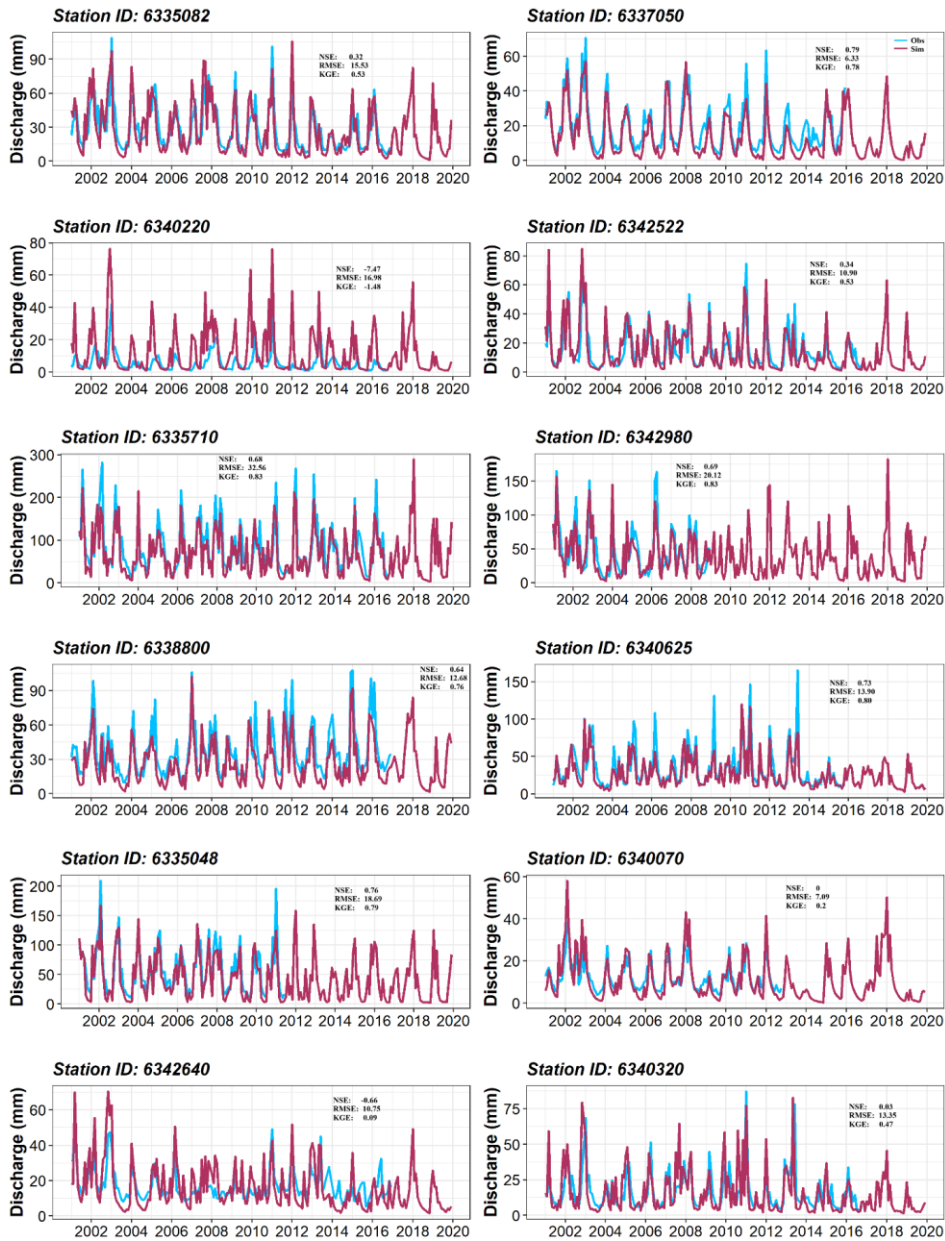
Deleted: were

Deleted: ed

Deleted: ed

Deleted: Furthermore, the hydrograph plots revealed that the model, in general, was able to simulate the monthly flows reasonably well, as shown in Fig. 2.

Deleted: wa



454 **Figure 2:** Monthly discharge time series from WaSSI simulation in mm (maroon) plotted against observed gauge
455 station flow in mm (blue) during 2000-2020.

456 3.1.2. ET Validation

457 Monthly land cover specific validation of simulated ET against EC ET is presented in Fig. 3. The ET estimates are
458 captured reasonably well by the model as the points in the scatter plot generally stayed close to the 1:1 line except for
459 Grassland. The detailed validation results are provided in Table S5. Ten out of eleven watersheds have an R^2 value $>$
460 0.6 and a correlation $>$ 0.75. Seven out of eleven watersheds have a model bias (%) between -25% to 25%, and KGE
461 estimate \geq 0.6. Discrepancies are found in Lackenberg station with a bias of 52.4 %, and in general we observed that
462 WaSSI model tends to slightly overestimate ET during winter. Overall, the model is able to capture ET values
463 reasonably well across different land covers within Germany (Fig. S2a).

464 WaSSI ET on an interannual scale showed that it can satisfactorily simulate the variability of ET captured by MODIS
465 across Germany, as shown in Fig S2b-c. The model mostly underestimated ET in southern and northwestern Germany,
466 while slightly overestimating the ET in mid-western and eastern Germany. When the simulated ET is assessed against
467 ET estimates as precipitation minus observed discharge ($P - Q_{\text{observed}}$) interannually, the mean annual biases for all the
468 twelve watersheds are within $\pm 25\%$ threshold. Eight out of the twelve watersheds have biases within $\pm 10\%$, indicating
469 a very good model performance (Table S6).

Deleted: ¶

Deleted: The ET estimates from WaSSI were compared with multiple eddy flux (EC) ET observations that are available within Germany. ...

Deleted: were

Deleted: d

Deleted: d

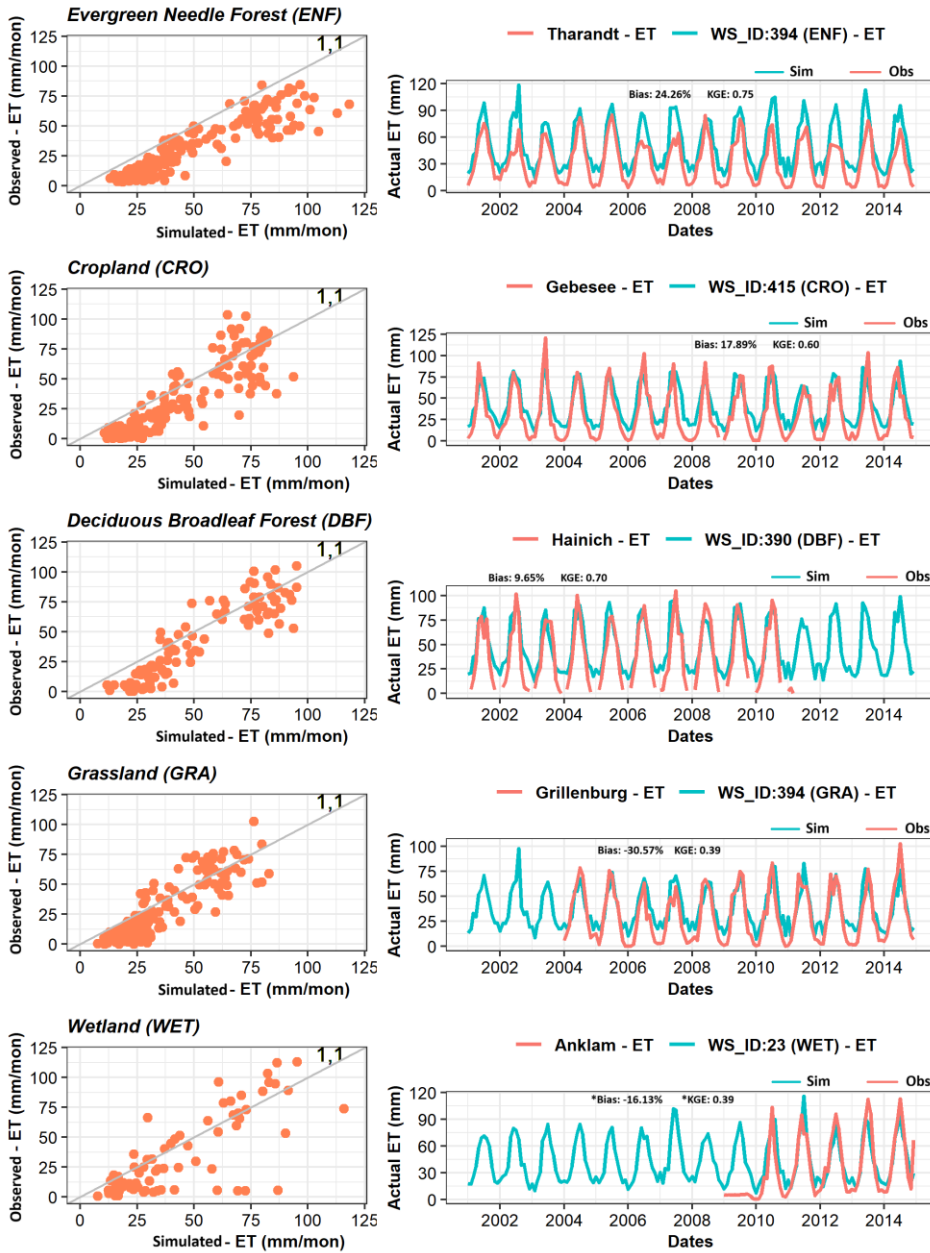
Deleted: The greatest discrepancy in this validation was

Deleted: wa

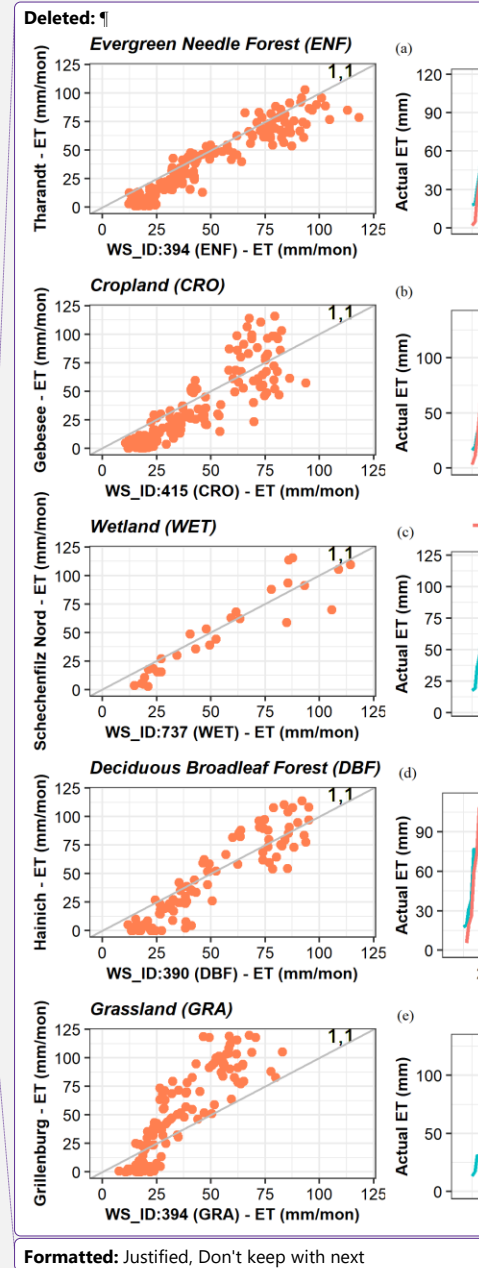
Deleted: wa

Deleted: were

Deleted: d



484



Formatted: Justified, Don't keep with next

487 **Figure 3:** Land cover specific simulated ET validation (WS_ID) against corrected eddy flux ET data. The line running
 488 diagonally through the scatter plot is a 1:1 line. The performance metrics provided were calculated using corrected
 489 ET for all stations except for Anklam (wetland).

490 **3.1.3. GPP Validation**

491 The results showed that nine out of fourteen watersheds have a model bias within $\pm 25\%$, twelve had $R^2 > 0.6$, seven
 492 had $NSE > 0.5$, six have $KGE > 0.5$, and all the watersheds have a correlation > 0.6 , as shown in Table 1. Furthermore,
 493 the results show that simulated GPP from WaSSI are higher compared to the remotely sensed GPP estimates from
 494 Copernicus and MODIS satellite by approximately 7% and 16%, respectively. The difference, correlation and
 495 regression between simulated GPP and remotely sensed GPP is shown in Fig. S3.

496 **Table 1:** Monthly validation of WaSSI-GPP against EC-GPP. Stations are grouped for different land covers e.g.
 497 cropland (CRO), deciduous broadleaf forest (DBF), ENF, grassland (GRA) and wetland (WET).

498

Eddy Flux Tower	Watershed ID	Land cover	Model bias %	R ²	Corr	NSE	KGE
Selhausen Juelich	457	CRO	-15.94	0.65	0.81	0.45	0.33
Klingenberg	394		8.34	0.38	0.62	0.37	0.37
Gebsee	415		13.54	0.48	0.69	0.41	0.35
Hainich	390	DBF	8.28	0.84	0.92	0.73	0.57
Leinefelde	390		3.19	0.87	0.93	0.75	0.57
Lackenberg	631		224.09	0.83	0.91	-5.82	-1.51
Oberbärenburg	394	ENF	-13.4	0.86	0.93	0.74	0.59
Tharandt	394		-19.7	0.89	0.94	0.73	0.59
Grillenbug	394	GRA	-35.42	0.75	0.87	0.37	0.3
Rollebroich	457		-26.79	0.81	0.9	0.55	0.49
Schechenfilz Nord	737		2.61	0.68	0.83	0.67	0.82
Spreewald	269	WET	-50.54	0.82	0.91	0.18	0.16
Zarnekow	38		21.62	0.84	0.92	0.77	0.7
Anklam	23		-40.91	0.63	0.79	0.28	0.2

499

Deleted: A monthly land cover specific validation was conducted between modelled GPP and observed GPP from EC towers. The observed GPP estimates were developed using the daytime partitioning method (GPP_DT_VUT_REF). ...

Deleted: d

Deleted: d

Deleted: d

Deleted: ed

Deleted: were

510 **3.2. Understanding the water-carbon coupling across Germany**

511 **3.2.1. Spatial variation of ET from 2001 - 2019**

512 Over a nineteen-year period, the mean annual ET across Germany ranges between 250 to 800 mm yr⁻¹ and has a spatial
513 mean and standard deviation of 530 ± 49.5 mm yr⁻¹. Eastern Germany (Saxony Anhalt, Brandenburg, Mecklenburg
514 Vorpommern, Saxony, and Thuringia) have lower ET than the spatial mean, while the South and West has higher ET,
515 as shown in Fig. 4a. On an annual scale, Bavaria and Lower Saxony experiences significant ET losses. The absolute
516 losses are 39.5 billion m³ yr⁻¹ in Bavaria and 25.7 billion m³ yr⁻¹ in Lower Saxony. Bavaria has a smaller fraction of
517 its precipitation lost as ET (0.3 to 0.9) compared to Lower Saxony (0.5 to 0.9). Across Germany, the eastern states
518 lost the largest share of their precipitation as ET (0.8 – 1.0), leading to a very limited available water supply in the
519 region, shown in Fig. 4b. Furthermore, to understand whether ET is limited by energy or water availability, we
520 estimated ET:PET ratio across Germany. PET is the atmospheric evaporative demand under ideal conditions (i.e., no
521 soil water stress) and acts as an upper limit of ET. The actual ET of watersheds near the Alps exceeds the PET due to
522 high precipitation, saturated soils and land cover type. These watersheds receive more precipitation compared to the
523 rest therefore, energy limits the ET values, while, for the rest parts of Germany the water availability limits ET (Fig.
524 4c). Lastly, eastern states and some watersheds in Rhineland-Pfalz and Hessen are drier with relatively high-water
525 scarcity as they receive less precipitation compared to their PET (Fig. 4d).

Deleted: ed

Deleted: d

Deleted: d

Deleted: d

Deleted: d

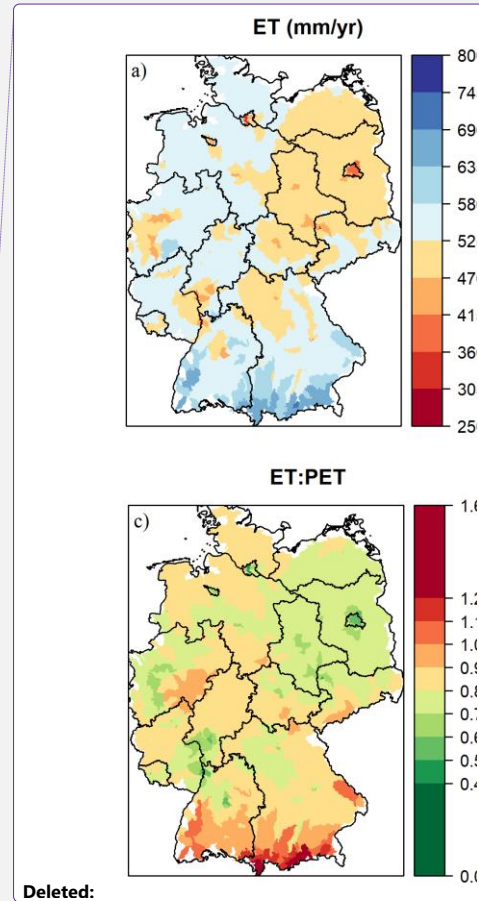
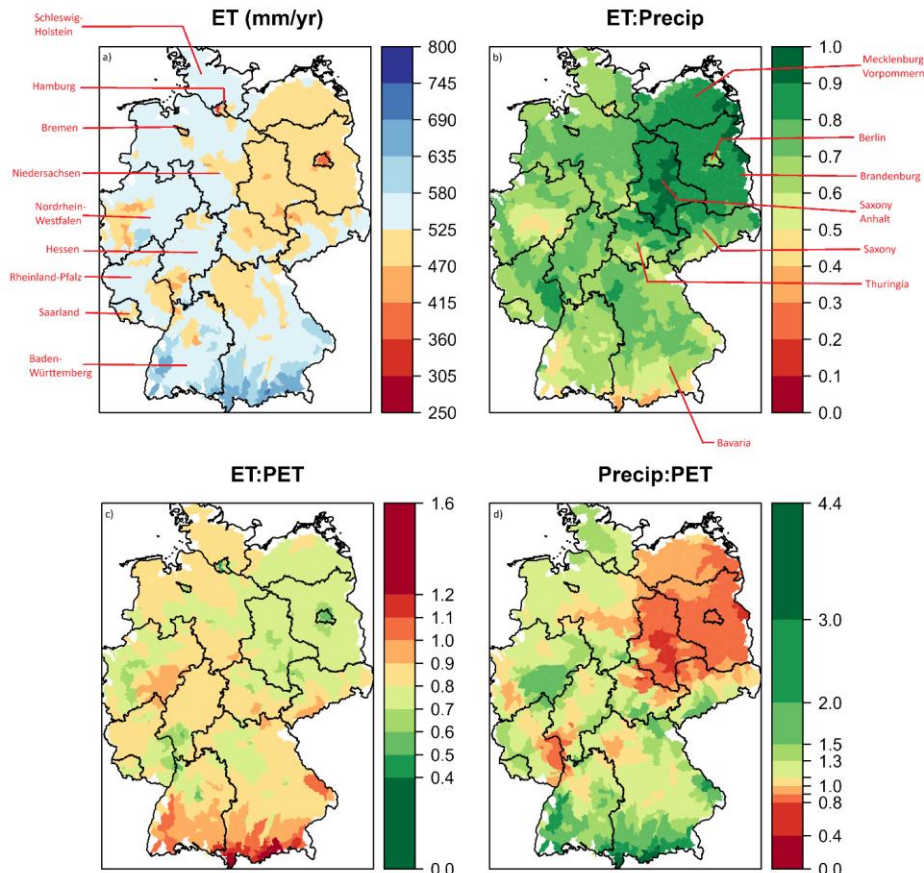
Deleted: were

Deleted: d

Deleted: and

Deleted: us

Deleted: the water availability limits ET



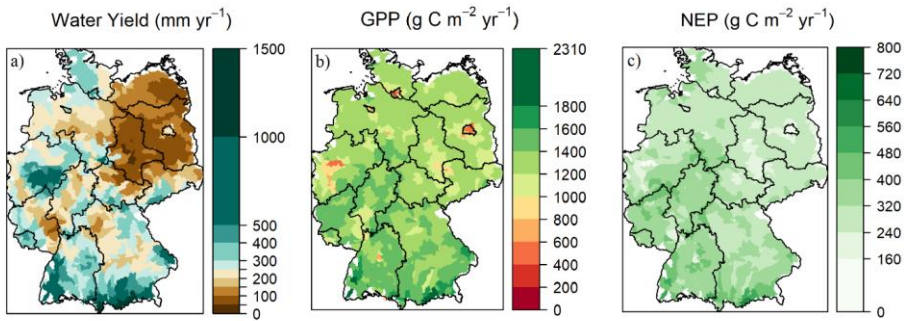
536

537 **Figure 4:** Modelled parameters presenting ET dynamics on a watershed scale across Germany over state boundaries
 538 within the period of 2001 - 2019. The separate sections show a) mean annual actual ET (mm yr⁻¹), b) ratios between
 539 ET and precipitation, c) ratios between the ET and potential ET and d) ratios between precipitation and potential ET.

540 **3.2.2. Ecosystem services across Germany throughout 2001 – 2019.**

541 The mean annual water yield across Germany ranges between 31.8 – 1477.5 mm yr⁻¹, has a spatial average of 259 ±
 542 173.5 mm yr⁻¹ and generates a total discharge of 84.86 billion m³ per year (Fig. 5a). In eastern states the water yield
 543 is lower than the spatial average, while in southern states it is higher. The mean annual GPP estimates (Fig. 5b) are
 544 found between 0 – 2046.5 g C m⁻² yr⁻¹ with a spatial average of 1278.8 ± 237.7 g C m⁻² yr⁻¹ and a total national carbon
 545 uptake of 441.54 Tg C yr⁻¹. The mean annual NEP values (Fig. 5c) are observed between 0 – 665.5 g C m⁻² yr⁻¹ with
 546 a spatial average of 308.3 ± 78.2 g C m⁻² yr⁻¹ and a total national carbon sequestration of 106.03 Tg C yr⁻¹.

Deleted: wa
 Deleted: wa
 Deleted: were
 Deleted: were



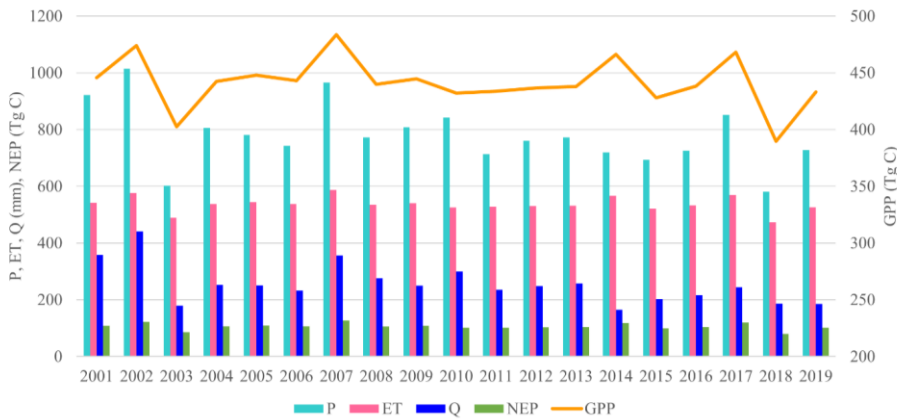
552

553 **Figure 5:** Spatial distribution of model simulated a) mean annual total water yield (mm yr⁻¹), b) mean annual GPP (g C
554 m⁻² yr⁻¹), and c) mean annual NEP (g C m⁻² yr⁻¹).

555 **3.2.3. Temporal variability of ecosystem services and the control of land cover on these services.**

556 The mean annual precipitation for the period 2001–2019 is estimated at 779 ± 106.2 mm/year. Notably, 2002 and
557 2007 are identified as the two wettest years within this timeframe. Precipitation in 2002 exceeded the mean by 30.2%,
558 while in 2007 it was 24% higher than the mean. Conversely, the driest years are 2003 and 2018, with rainfall falling
559 below the mean by 22.7% and 25.5%, respectively. There are relatively high variations in Q and NEP during these
560 wet and dry years, indicating that these two fluxes are sensitive to changes in precipitation compared to ET and GPP.
561 In 2018, which is the driest year in the study period, we observed that compared to the mean there is 25.5% less
562 precipitation. This is accompanied by 11.7% less ET, a 26.8% reduction in Q, 11.7% less GPP and 24.7% lower NEP.
563 Alternatively, during 2002, the wettest year in our study, we found 30.2% more precipitation compared to mean.
564 Which may have led to 7.4% more in ET, 73.4% higher Q, 7.3% more GPP, and 15.5% rise in NEP, relative to mean.
565 An annual overview for temporal variation is presented in Fig. 6.

Deleted: wa
Deleted: were
Deleted: was
Deleted: were
Deleted: were
Deleted: was
Deleted: was

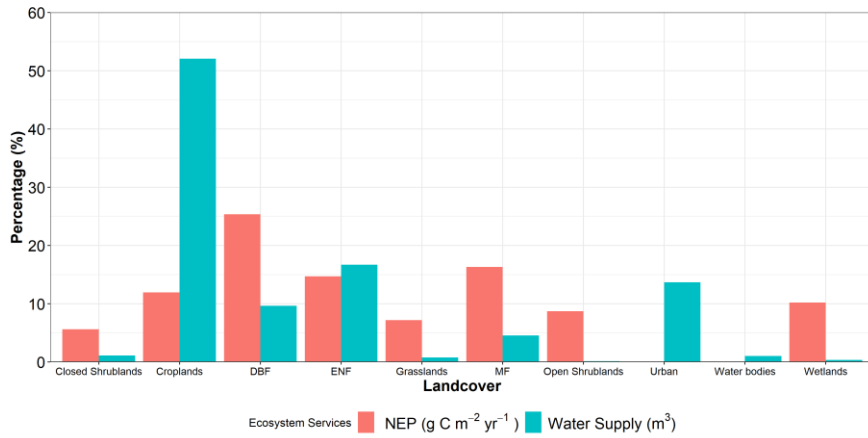


566

567 **Figure 6:** Simulated annual ecosystem fluxes evapotranspiration ET (mm), Net ecosystem productivity NEP (Tg C)
568), Gross Primary Productivity GPP (Tg C), discharge Q (mm), and precipitation P (mm) across Germany simulated
569 by the model during 2001 - 2019.

Deleted: E
Deleted: (
Deleted: Precipitation,
Deleted: E
Deleted:)
Deleted: (
Deleted:)
Deleted:
Deleted: P
Deleted: from
Deleted: to observe annual variation

588 To evaluate the role of land cover in water yield and carbon sequestration, we estimated the share of ecosystem services
 589 provided by the ten different land cover classes. The most essential land covers that provide the largest share of water
 590 across Germany are Cropland (52.1%), ENF (16.7%), and Urban (13.7%); they supply 82.5% of the water in total.
 591 Furthermore, forest sequester most of the carbon, DBF (25.3%), mixed forest (MF) (16.3%), and ENF (14.7%). They
 592 contribute 56.3% of carbon sequestered in Germany while only accounting for 30.5% of the land cover. Lastly, we
 593 would like to highlight that a small portion of land covers, such as wetlands, open shrubland, closed shrubland, and
 594 grasslands cover less than 2% of German territory; however, they regulate > 30% of the total carbon sequestered in
 595 Germany, indicating the high importance of conserving these ecosystems, as shown in Fig. 7.



596
 597 **Figure 7:** Simulated mean percentage or share of carbon sequestration and water supply originating from different
 598 land covers across Germany.

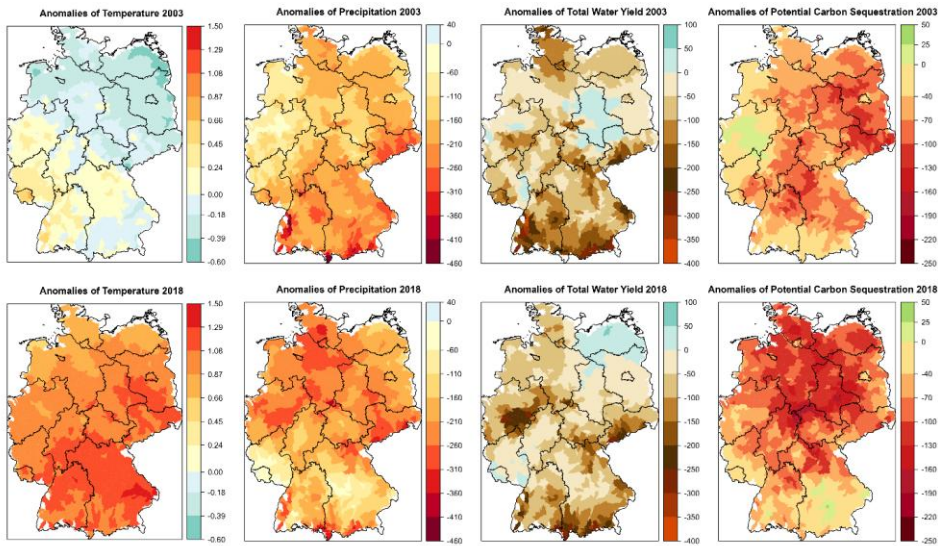
599 **3.2.4. Spatial variability of ecosystem services during extreme weather events**

600 To understand the impact of droughts and extreme precipitation on ecosystem services, we examined the droughts for
 601 the year 2003 & 2018 and the extremely wet years 2002 and 2013. During 2003, precipitation was 22.7% less than its
 602 average and only western states had close to average precipitation. The total water yield was 29.6% less than average.
 603 The carbon sequestration was 18.5% lower than average. While western states had close to average carbon
 604 sequestration the rest experienced significantly reduced levels. Compared to 2003, the pattern and intensity of the
 605 2018 drought was more severe. During this event, Germany cumulatively received 25.5% less precipitation, had a
 606 26.8% lower water yield, and had 24.7% less carbon sequestration. The total water yield was 62.13 billion m³, total
 607 carbon uptake was 389.77 TgC, and total carbon sequestration was 79.82 TgC. The variations in ecosystem services
 608 due to both drought events are presented in Fig. 8. On the other hand, during the extremely wet year of 2002, Germany
 609 received 30% more precipitation than annual mean. The water yield and carbon sequestration were 70% and 15.5%
 610 higher than the mean, respectively. The second wet year of 2013 suffered from severe regional floods. The regions
 611 that received higher precipitation had a larger water yield and sequestered more carbon. Interestingly, northwest
 612 Germany was drier than the mean, as a result, the overall ecosystem services for 2013 were close to the mean estimates.
 613 The variations in ecosystem services during both years are presented in Fig. 9.

Deleted: The land covers that
 Deleted: are
 Deleted: ;
 Deleted: t

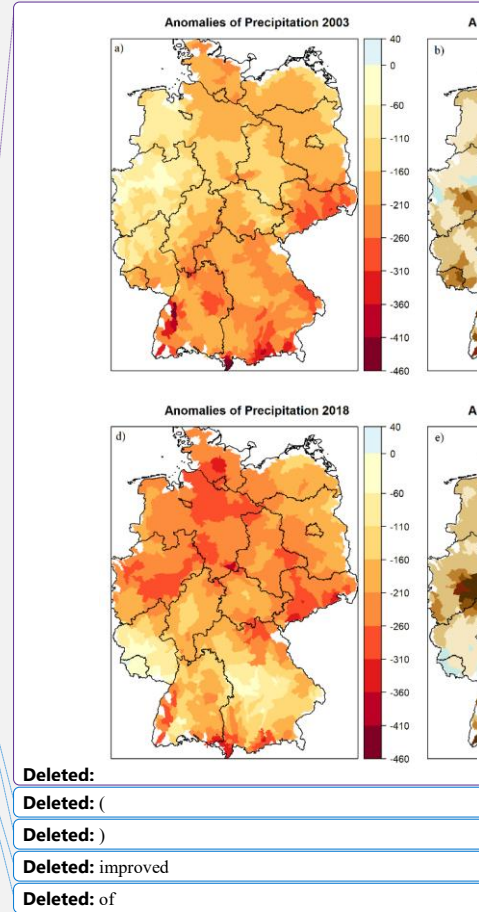
Deleted: The

Deleted: floods
 Deleted: floods for the



621
622
623
624
625
626

Figure 8: The response of ecosystem services, water yield (mm) and carbon sequestration (g C m^{-2}), during two drought events (2003 and 2018). Both drought events had different spatial patterns and intensities, thus the response from the ecosystem varied spatially. The anomalies in the figure were estimated by subtracting the mean annual values for the period 2001 – 2019 from the estimates of the individual drought years 2003 and 2018 on a watershed scale. The temperature anomalies ($^{\circ}\text{C}$) are also provided for understanding the events.



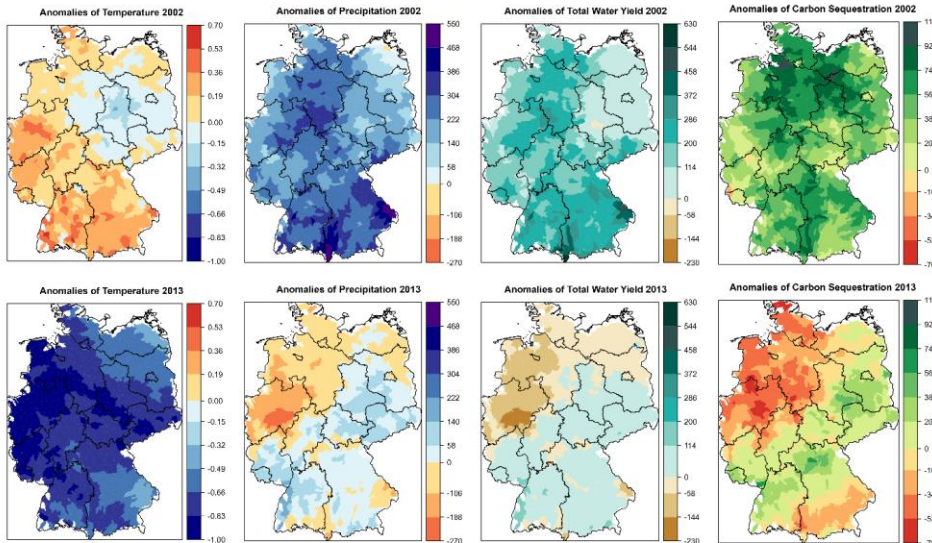
Deleted:

Deleted: (

Deleted:)

Deleted: improved

Deleted: of



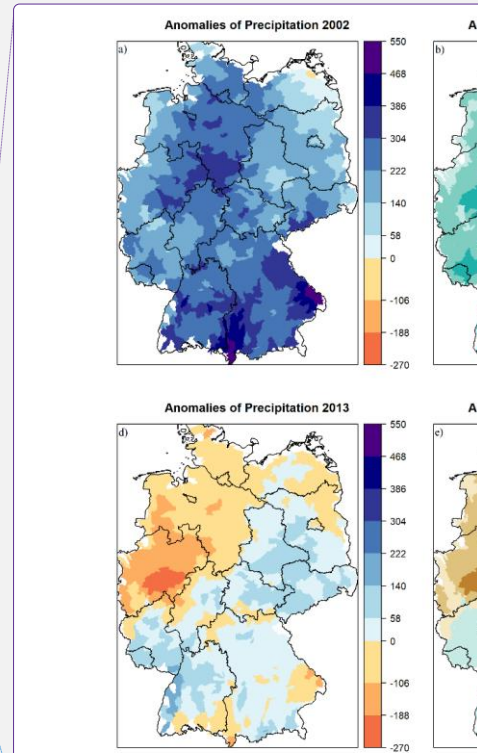
632
 633 **Figure 9:** The response of ecosystem services, water yield (mm) and carbon sequestration (g C m^{-2}), during two
 634 extreme precipitation events (2002 and 2013). Both events had different spatial patterns and intensities, thus the
 635 response from the ecosystem varied spatially. The anomalies in the figure were estimated by subtracting the mean
 636 annual values for the period 2001 – 2019 from the estimates of the individual years 2002 and 2013 on a watershed
 637 scale. The temperature anomalies ($^{\circ}\text{C}$) are also provided for understanding the events.

638 **4. Discussion**

639 This study explores the response of water-carbon cycle to land cover and extreme events across Germany on watershed
 640 scale. The WaSSI model performs reasonably well in this region and is estimated to generate 84.86 billion m^3 of
 641 discharge and 106.03 TgC of carbon sequestration per year. The results (Figure 7) also highlight the importance of
 642 sparse landcovers (e.g. wetlands, open shrubland, closed shrubland, and grasslands) in regulating carbon sequestration.
 643 Furthermore, the study shows that ecosystem services are quite sensitive to droughts and extreme precipitation events,
 644 but buffers developed from the previous year can play a significant role in mitigating this effect. As shown in Figure
 645 8, we observe low but positive water yield anomalies during drought years in parts of Germany. Buffers can help delay
 646 the onset of hydrological droughts in the region.

647 The model validation results successfully demonstrate that the model can be applied across Germany. Furthermore,
 648 due to the common climatic and hydrological regime, we believe the model can potentially be applied to a broader
 649 central European region. The simulated discharge had small model bias percentage and high regression values.
 650 Furthermore, the spatial and temporal variability of the discharge was modelled reasonably well with high NSE, KGE,
 651 R^2 and low P-bias for most watersheds (Table S3 - S4). Except for station Wasserthaleben, which had very high flow
 652 values leading to a P-bias equal to 131.8%, KGE of -1.48, and annual R^2 of 0.18. The poor performance of this
 653 individual station could be attributed to several possible reasons, including its relatively small surface area, the
 654 uncertainty of input data (soil parameters or climate data), underestimation of losses to groundwater, simplification of
 655 physical processes that estimate surface runoff, or the presence of prevalent unidentified dams in the watershed
 656 (Caldwell et al., 2012).

657 Simulated ET validated reasonably well against data from different eddy flux towers across the study area (Fig. 3).
 658 The largest discrepancy was found in Lackenberg station. Even though corrected ET values are used for validation,
 659 there might be uncertainties in correction factor (Pastorello et al., 2020), and inaccuracies in the observed data due to



- Deleted:
- Deleted: (
- Deleted:)
- Deleted: flood
- Deleted: year
- Deleted: improved
- Deleted: of
- Deleted: from
- Deleted: floods
- Deleted: central Europe (e.g. Germany)

Deleted: (Caldwell et al., 2012)

Deleted: (Pastorello et al., 2020)

672 energy imbalance. For spatial analysis, the simulated ET was compared with MODIS data. The model values were
673 low compared to MODIS ET in southern and northwestern Germany, but high in mid-western and eastern Germany.
674 The discrepancies between MODIS-ET and WaSSI ET could be attributed to multiple factors, i.e. the intrinsic
675 limitations of the different algorithms used by the model and MODIS to estimate ET, uncertainty from the
676 misclassification of land cover between the two datasets, uncertainties in the model's input data, uncertainties in
677 MODIS's input data, exclusion of waterbodies in ET estimation by MODIS, and the role of interception in MODIS-
678 ET estimation (Kim et al., 2012; Trambauer et al., 2014).

679 Furthermore, the model performance across different land covers showed that simulated GPP estimates capture forest
680 biomes significantly well, except for the station in Lackenberg Forest. The model performance for the rest of the land
681 covers was less straightforward. For example, croplands had good model biases but low regression values; grasslands
682 had poor model biases, but high regression estimates; wetlands are more multifaceted (see Table 1). The discrepancies
683 in the results can be from 1) the model's inherent limitation i.e., lack of radiation in model PET leading to
684 underestimation of GPP, 2) an insufficient number of eddy flux data for different land covers, and uncertainty in eddy
685 flux GPP. The uncertainty of daily GPP can reach 15% to 20% (Falge et al., 2002; Hagen et al., 2006; Lasslop et al.,
686 2010; Verma et al., 2014). Understanding uncertainties in eddy flux GPP is ongoing research. The mismatch of land
687 cover and landscape heterogeneity at the evaluation sites between the model (watershed scale) and the eddy flux
688 (single location) will reduce as more data becomes available with time (Verma et al., 2014). Lastly, the difference
689 between spatial distribution of simulated GPP and remotely sensed GPP may be due to WUE parameters. They were
690 derived from the global FLUXNET database, which might not have sufficient representation of certain ecosystems
691 (e.g., wetlands and savannas) resulting in a bias of GPP estimation (Sun et al., 2011). Nevertheless, multiple studies
692 have also shown that data from remote sensing tends to underestimate GPP (Liu et al., 2015; Wang et al., 2017; Zhu
693 et al., 2018).

694 The simulated stocks and flows of ecosystem services across Germany by this study were similar to Zink et al. (2016),
695 and Huang et al. (2010), who reported annual ET and water scarcity patterns at individual sites. The eastern region
696 in Germany generally receives less precipitation, has high mean annual temperature, high ET from forests and low
697 water yield, implying intense water use competition. The total water supply reported by German Environment Agency
698 (UBA) was higher than the simulated results because WaSSI model does not consider transboundary flows (J. Arle et
699 al., 2018). Furthermore, the southern region in Germany had slightly higher carbon uptake and sequestration values
700 than the rest of the country. The distribution patterns of carbon sequestration were similar to carbon uptake because
701 NEP and GPP have a linear relationship. Urban areas sequestered limited carbon but played a significant role in
702 altering water balances. The distribution and management of land use and land cover determine how ecosystem
703 services vary. To ensure adequate quantity and quality of services, like freshwater and natural sink of CO₂, land use
704 decision-making must incorporate the assessment of currently available stocks and their actual value according to
705 regional and national priorities. Based on historical data, the available stocks quantified in this study provide evidence
706 to relevant stakeholders of different regions. Furthermore, the significance of minor land covers or ecosystems in
707 terms of proportional coverage, such as wetlands, is also highlighted. Germany aims to become CO₂ neutral by 2045;
708 synergies and tradeoffs of ecosystem services can be used to design land use policy that align with Sustainable
709 Development Goals. A science-based approach will be necessary to leverage the potential of natural C sink to fix and
710 offset carbon emissions.

711 As the frequency and intensity of periodic dry and wet spells change due to global warming so does their impact
712 through drought and extreme precipitation events. In this work, we, quantified the response of water yield and carbon
713 sequestration to extreme drought and high precipitation events across Germany. During the drought events of 2003
714 and 2018, the lack of precipitation, overall, had a direct negative impact on water yield and carbon sequestration. But
715 it is interesting to see that soil has stored water from the previous years, acting as a buffer and provide limited relief
716 during extreme drought events (Fig. 8). According to Ciaia et al. (2005), a 30% reduction in carbon uptake was
717 observed across Europe during the drought of 2003, while we estimated a reduction of around 8.8% for Germany.
718 Europe-wide studies on the impacts of the 2018 drought event on carbon sequestration are presented by Thompson et
719 al. (2020), and Smith et al. (2020). They found that the annual sequestration anomaly in 2018 across northern Europe
720 was 0.02 ± 0.02 PgC yr⁻¹ less compared to a 10-year European mean (Thompson et al., 2020). It was estimated that
721 during the year 2018 an overall reduction in sequestration was around 57 TgC (Smith et al., 2020). However, a direct
722 comparison between our research is difficult due to the difference in the spatial boundaries. In general, Germany has
723 no shortage of water, however, a trend to have less precipitation during summer seasons or prolonged dry spells during

Deleted: (Kim et al., 2012; Trambauer et al., 2014)

Deleted: complex, but reasonable

Deleted: complicated

Deleted: (Falge et al., 2002; Hagen et al., 2006; Lasslop et al., 2010; Verma et al., 2014)

Deleted: (Verma et al., 2014)

Deleted: (Sun et al., 2011)

Deleted: (Liu et al., 2015; Wang et al., 2017; Zhu et al., 2018)

Deleted: model helps determine the

Deleted: . W

Deleted: e found that

Deleted: Zink et al. (2016)

Deleted: Huang et al. (2010)

Deleted: estimated similar

Deleted: across Germany in

Deleted: their

Deleted: studies

Deleted: take into account

Deleted: in

Deleted: (J. Arle et al., 2018)

Deleted: did not

Deleted: any

Deleted: providing water supply

Deleted: flood

Formatted: Font: (Default) Times New Roman

Deleted: is able to

Deleted: which

Deleted: Ciaia et al. (2005)

Deleted: Thompson et al. (2020)

Deleted: Smith et al. (2020)

Deleted: (Thompson et al., 2020)

Deleted: (Smith et al., 2020)

756 main vegetation growing months can have substantial adverse effects on both surface water and groundwater supply.
757 Temporary seasonal rainfall deficiency can cause significant losses of surface water supply and carbon sequestration,
758 leading to dry conditions that negatively affect the yields and products from the agriculture and forestry sectors. For
759 example, low soil water availability weakens forest health and favors bark beetle infestation, resulting in huge
760 economic losses of timber values and forest areas in Germany over the last few years (Lausch et al., 2013;
761 Zimmermann & Hoffmann, 2020), and the situation continues to worsen. Therefore, land use transformation to adapt
762 to climate change is indispensable to developing ecological resiliency based on an improved understanding of the role
763 of various land covers in providing ecosystem services.

764 While this study provides valuable insights on response of water-carbon cycle to land cover and extreme events, it is
765 limited by the scope of WaSSI Model. The monthly temporal resolution of the model prevents it from estimating peak
766 flows accurately. The use of WUE to connect ET and carbon sequestration is limited due to insufficient eddy flux
767 tower coverage. The lack of transboundary river flow and omission of crop rotation further limits the application of
768 this model. In future, we plan to use WaSSI model across hydrological boundaries, apply projected climate data and
769 projected landcover data to run simulations for different scenarios. The analysis will help us evaluate future changes
770 in ecosystem services.

771 5. Conclusions

772 This study presents new insights into the relationship between water-carbon cycle and land cover, and the impacts of
773 climate extremes across Germany. The model validation results holistically show that the simple water and carbon
774 model could capture ecosystem services reasonably well at the national level. Furthermore, the spatial and temporal
775 relationship between carbon and water highlighted that the eastern states of Germany are comparatively drier than the
776 rest of the country because most of their precipitation is lost as ET. Nationally, ecosystems in Germany generates a
777 total annual discharge of 84.86 billion m³ and sequester 106Tg C yr⁻¹ carbon. Croplands supply the largest percentage
778 of available water, while forests sequester the major share of carbon. Minor land covers (e.g. wetlands, open
779 shrubland, closed shrubland, and grasslands) are also very important in providing ecosystem services for carbon
780 sequestration. The extreme events in 2003 and 2018 had a significant impact on ecosystem services at the national
781 level. Moreover, the severe flood of 2013 also played a major role on a regional scale in the Elbe and Danube River
782 basins. This rigorously verified model provides confidence that the model can be used to strategic applications for
783 developing Nature-based Solutions (NbS), which will be helpful for Germany to meet its net-zero carbon emissions
784 by 2050.

Formatted: Font: (Default) Times New Roman, 10 pt,
Font color: Black

Deleted: (Lausch et al., 2013; Zimmermann & Hoffmann,
2020)

Deleted: The average

Deleted: water yield across Germany ranges from 32 – 1478
mm yr⁻¹ and

Deleted: per year. Similarly, the average

Deleted:

Deleted: carbon sequestration ranges from 0 – 666 g C m⁻²
yr⁻¹ and annually sequesters

Deleted: .

Deleted: Our simulation results showed that

Deleted: c

Deleted: DBF

Deleted: The analysis also emphasized the critical role of

Deleted: m

Deleted: In the future, we aim to concentrate our research
efforts on understanding how land use land cover change or
landscape transformation will affect water yield and carbon
sequestration across different watersheds for climate
adaptation. ...

805 **6. Acknowledgment**

806 This work was supported by the German Academic Exchange Service (DAAD) PPP Grant (Projekt-ID: 57510261).
807 We appreciate the funding support from UNU-FLORES and the generous support provided by the US partner – the
808 Southern Research Station of the United States Forest Service. We also would like to thank the Thünen Institute of
809 Forest Ecosystems for collaboration.

810 **7. Data Availability**

811 Model software ([Liu, 2021](#)), output data ([Pyarali, 2024b](#)), and corresponding watershed shapefile ([Pyarali, 2024a](#)), used
812 and prepared in this study are available open source via figshare and can be access from the links in reference list.

813 **8. Author Contributions**

814 *Karim Pyarali*: Writing, review & editing manuscript, Methodology, Investigation, Data curation, Conceptualization.
815 *Lulu Zhang*: Review, Supervision, Methodology, Funding acquisition, Conceptualization. *Ge Sun*: Review,
816 Supervision, Methodology, Conceptualization. *Ning Liu*: Review, Data curation, Methodology. *Abdulhakeem Al-*
817 *Qubati*: Review, Data curation, Methodology.

818 **9. Competing Interests:**

819 The authors declare that they have no known competing financial interests or personal relationships that could have
820 appeared to influence the work reported in this paper.

Deleted: (Liu, 2021)

Deleted: (Pyarali, 2024b)

Deleted: (Pyarali, 2024a)

824 **10. Reference**

- 825 | Allan, A., Soltani, A., Abdi, M. H., & Zarei, M. (2022). Driving Forces behind Land Use and Land Cover Change: A
826 Systematic and Bibliometric Review. *Land*, 11(8), 1222. <https://doi.org/10.3390/land11081222>
- 827 Al-Qubati, A., Zhang, L., & Pyarali, K. (2023). Climatic drought impacts on key ecosystem services of a low mountain
828 region in Germany. *Environmental Monitoring and Assessment*, 195(7), 800. [https://doi.org/10.1007/s10661-](https://doi.org/10.1007/s10661-023-11397-1)
829 023-11397-1
- 830 Anderson, R. M., Koren, V. I., & Reed, S. M. (2006). Using SSURGO data to improve Sacramento Model a priori
831 parameter estimates. *Journal of Hydrology*, 320(1–2), 103–116.
832 <https://doi.org/10.1016/J.JHYDROL.2005.07.020>
- 833 Arowolo, A. O., Deng, X., Olatunji, O. A., & Obayelu, A. E. (2018). Assessing changes in the value of ecosystem
834 services in response to land-use/land-cover dynamics in Nigeria. *Science of The Total Environment*, 636, 597–
835 609. <https://doi.org/10.1016/j.scitotenv.2018.04.277>
- 836 Averyt, K., Fisher, J., Huber-Lee, A., Lewis, A., Macknick, J., Madden, N., Rogers, J., & Tellinghuisen, S. (2011).
837 *Freshwater Use by U.S. Power Plants. Electricity's Thirst for a Precious Resource*.
- 838 Beer, C., Reichstein, M., Ciais, P., Farquhar, G. D., & Papale, D. (2007). Mean annual GPP of Europe derived from
839 its water balance. *Geophysical Research Letters*, 34(5). <https://doi.org/10.1029/2006GL029006>
- 840 Brown de Colstoun, E. C., C. Huang, P. Wang, J. C. Tilton, B. Tan, J. Phillips, S. Niemczura, P.-Y. Ling, & R. E.
841 Wolfe. (2017). *Global Man-made Impervious Surface (GMIS) Dataset From Landsat, v1: Global High*
842 *Resolution Urban Data from Landsat*. Palisades, NY: NASA Socioeconomic Data and Applications Center
843 (SEDAC).
- 844 Büttner, G., Kosztra, B., Maucha, G., Pataki, R., Kleeschulte, S., Hazeu, G., Vittek, M., Schröder, C., & Littkopf, A.
845 (2021). *Copernicus Land Monitoring Service CORINE Land Cover (User Manual)*.
846 <https://land.copernicus.eu/pan-european/corine-land-cover/clc2018?tab=mapview>
- 847 Caldwell, P., Muldoon, C., Ford-Miniat, C., Cohen, E., Krieger, S., Sun, G., McNulty, S., & Bolstad, P. V. (2014).
848 *Quantifying the role of National Forest System lands in providing surface drinking water supply for the Southern*
849 *United States*. <https://doi.org/10.2737/SRS-GTR-197>
- 850 Caldwell, P., Sun, G., McNulty, S. G., Cohen, E., & Moore Myers, J. a. (2011). Modeling impacts of environmental
851 change on ecosystem services across the conterminous United States. *The Fourth Interagency Conference on*
852 *Research in the Watersheds*, Fairbanks, AK, USA.
853 http://admin.forestthreats.org/products/publications/Modeling_impacts_of_environmental_change.pdf
- 854 Caldwell, P. V., Sun, G., McNulty, S. G., Cohen, E. C., & Moore Myers, J. A. (2012). Impacts of impervious cover,
855 water withdrawals, and climate change on river flows in the conterminous US. *Hydrology and Earth System*
856 *Sciences*, 16(8), 2839–2857. <https://doi.org/10.5194/hess-16-2839-2012>
- 857 Camacho, F., & Cernicharo, J. (2014). Gio Global Land Component - Lot I "Operation of the Global Land
858 Component". In *Algorithm Theoretical Basis Document, Issue II.01*.
859 http://land.copernicus.eu/global/sites/default/files/products/GIOGL1_ATBD_SAV1_II.01.pdf
- 860 Chen, D., Liu, N., Gan, G., Liu, Y., Qin, M., Zheng, Q., Sun, G., & Hao, L. (2024). Combined effects of urbanization
861 and climate variability on water and carbon balances in a rice paddy-dominated basin in southern China.
862 *Environmental Research Letters*, 19(12), 124042. <https://doi.org/10.1088/1748-9326/ad8a73>
- 863 Cheng, L., Zhang, L., Wang, Y. P., Canadell, J. G., Chiew, F. H. S., Beringer, J., Li, L., Miralles, D. G., Piao, S., &
864 Zhang, Y. (2017). Recent increases in terrestrial carbon uptake at little cost to the water cycle. *Nature*
865 *Communications* 2017 8:1, 8(1), 1–10. <https://doi.org/10.1038/s41467-017-00114-5>

Formatted: Italian (Italy)

- 866 Ciais, P., Reichstein, M., Viovy, N., Granier, A., Ogée, J., Allard, V., Aubinet, M., Buchmann, N., Bernhofer, C.,
867 Carrara, A., Chevallier, F., De Noblet, N., Friend, A. D., Friedlingstein, P., Grünwald, T., Heinesch, B.,
868 Keronen, P., Knohl, A., Krinner, G., ... Valentini, R. (2005). Europe-wide reduction in primary productivity
869 caused by the heat and drought in 2003. *Nature* 2005 437:7058, 437(7058), 529–533.
870 <https://doi.org/10.1038/nature03972>
- 871 Cui, F., Wang, B., Zhang, Q., Tang, H., De Maeyer, P., Hamdi, R., & Dai, L. (2021). Climate change versus land-use
872 change—What affects the ecosystem services more in the forest-steppe ecotone? *Science of The Total*
873 *Environment*, 759, 143525. <https://doi.org/10.1016/j.scitotenv.2020.143525>
- 874 Donmez, C., Sahingoz, M., Paul, C., Cilek, A., Hoffmann, C., Berberoglu, S., Webber, H., & Helming, K. (2024).
875 Climate change causes spatial shifts in the productivity of agricultural long-term field experiments. *European*
876 *Journal of Agronomy*, 155, 127121. <https://doi.org/10.1016/j.eja.2024.127121>
- 877 DWD. (2018). *Grids of monthly averaged daily air temperature (2m) over Germany*.
878 https://opendata.dwd.de/climate_environment/CDC/grids_germany/monthly/
- 879 EEA. (2021). *CLC 2018 — Copernicus Land Monitoring Service*. [https://land.copernicus.eu/pan-european/corine-](https://land.copernicus.eu/pan-european/corine-land-cover/clc2018)
880 [land-cover/clc2018](https://land.copernicus.eu/pan-european/corine-land-cover/clc2018)
- 881 Eisenreich, S. J. (2005). *Climate Change and the European Water Dimension. A report to the European Water*
882 *Directors 2005. EU Report No. 21553*. [https://cetesb.sp.gov.br/proclima/2005/05/09/climate-change-and-the-](https://cetesb.sp.gov.br/proclima/2005/05/09/climate-change-and-the-european-water-dimension-a-report-to-the-european-water-directors/)
883 [european-water-dimension-a-report-to-the-european-water-directors/](https://cetesb.sp.gov.br/proclima/2005/05/09/climate-change-and-the-european-water-dimension-a-report-to-the-european-water-directors/)
- 884 Falge, E., Baldocchi, D., Tenhunen, J., Aubinet, M., Bakwin, P., Berbigier, P., Bernhofer, C., Burba, G., Clement, R.,
885 Davis, K. J., Elbers, J. A., Goldstein, A. H., Grelle, A., Granier, A., Gumundsson, J., Hollinger, D., Kowalski,
886 A. S., Katul, G., Law, B. E., ... Wofsy, S. (2002). Seasonality of ecosystem respiration and gross primary
887 production as derived from FLUXNET measurements. *Agricultural and Forest Meteorology*, 113(1–4), 53–74.
888 [https://doi.org/10.1016/S0168-1923\(02\)00102-8](https://doi.org/10.1016/S0168-1923(02)00102-8)
- 889 Fang, Y., Sun, G., Caldwell, P., McNulty, S. G., Noormets, A., Domec, J., King, J., Zhang, Z., Zhang, X., Lin, G.,
890 Zhou, G., Xiao, J., & Chen, J. (2015). Monthly land cover-specific evapotranspiration models derived from
891 global eddy flux measurements and remote sensing data. *Ecohydrology*, 9(2), 248–266.
892 <https://doi.org/10.1002/eco.1629>
- 893 *Fourth Federal Forest Inventory 2022*. (2024). [https://www.bundeswaldinventur.de/vierte-bundeswaldinventur-](https://www.bundeswaldinventur.de/vierte-bundeswaldinventur-2022/vorwort)
894 [2022/vorwort](https://www.bundeswaldinventur.de/vierte-bundeswaldinventur-2022/vorwort)
- 895 Gentine, P., Green, J. K., Guérin, M., Humphrey, V., Seneviratne, S. I., Zhang, Y., & Zhou, S. (2019). Coupling
896 between the terrestrial carbon and water cycles—a review. *Environmental Research Letters*, 14(8), 083003.
897 <https://doi.org/10.1088/1748-9326/AB22D6>
- 898 Gutsch, M., Lasch-Born, P., Kollas, C., Suckow, F., & Reyer, C. P. O. (2018). Balancing trade-offs between ecosystem
899 services in Germany's forests under climate change. *Environmental Research Letters*, 13(4), 045012.
900 <https://doi.org/10.1088/1748-9326/aab4e5>
- 901 Hagen, S. C., Braswell, B. H., Linder, E., Frohling, S., Richardson, A. D., & Hollinger, D. Y. (2006). Statistical
902 uncertainty of eddy flux - Based estimates of gross ecosystem carbon exchange at Howland Forest, Maine.
903 *Journal of Geophysical Research Atmospheres*, 111(8), 1–12. <https://doi.org/10.1029/2005JD006154>
- 904 Hasan, S. S., Zhen, L., Miah, Md. G., Ahamed, T., & Samie, A. (2020). Impact of land use change on ecosystem
905 services: A review. *Environmental Development*, 34, 100527. <https://doi.org/10.1016/j.envdev.2020.100527>
- 906 Huang, S., Krysanova, V., Österle, H., & Hattermann, F. F. (2010). Simulation of spatiotemporal dynamics of water
907 fluxes in Germany under climate change. *Hydrological Processes*, 24(23), 3289–3306.
908 <https://doi.org/10.1002/HYP.7753>

- 909 J. Arle, H. Bartel, C. Baumgarten, A. Bertram, R. Wolter, G. Winkelmann-Oei, & C. Winde. (2018). *Water Resource*
910 *Management in Germany: Fundamentals, Pressures, Measures*.
911 <https://www.umweltbundesamt.de/en/publikationen/water-resource-management-in-germany>
- 912 Jin, K., Liu, N., Tang, R., Sun, G., & Hao, L. (2025). Quantifying Long Term (2000–2020) Water Balances Across
913 Nepal by Integrating Remote Sensing and an Ecohydrological Model. *Remote Sensing*, 17(11), 1819.
914 <https://doi.org/10.3390/rs17111819>
- 915 Jung, M., Reichstein, M., Schwalm, C. R., Huntingford, C., Sitch, S., Ahlström, A., Arneth, A., Camps-Valls, G.,
916 Ciais, P., Friedlingstein, P., Gans, F., Ichii, K., Jain, A. K., Kato, E., Papale, D., Poulter, B., Raduly, B.,
917 Rödenbeck, C., Tramontana, G., ... Zeng, N. (2017). Compensatory water effects link yearly global land CO₂
918 sink changes to temperature. *Nature* 2017 541:7638, 541(7638), 516–520. <https://doi.org/10.1038/nature20780>
- 919 Kaspar, F., Müller-Westermeier, G., Penda, E., Mächel, H., Zimmermann, K., Kaiser-Weiss, A., & Deuschländer, T.
920 (2013). Monitoring of climate change in Germany – data, products and services of Germany’s National Climate
921 Data Centre. *Advances in Science and Research*, 10(1), 99–106. <https://doi.org/10.5194/asr-10-99-2013>
- 922 Keil, M. (2017). *CORINE Land Cover products for Germany* (Number January).
923 [https://www.dlr.de/eoc/Portaldata/60/Resources/dokumente/6_anw_land/CORINE_Land_Cover_products_for](https://www.dlr.de/eoc/Portaldata/60/Resources/dokumente/6_anw_land/CORINE_Land_Cover_products_for_Germany_at_DFD.pdf)
924 [_Germany_at_DFD.pdf](https://www.dlr.de/eoc/Portaldata/60/Resources/dokumente/6_anw_land/CORINE_Land_Cover_products_for_Germany_at_DFD.pdf)
- 925 Kim, H. W., Hwang, K., Mu, Q., Lee, S. O., & Choi, M. (2012). Validation of MODIS 16 global terrestrial
926 evapotranspiration products in various climates and land cover types in Asia. *KSCCE Journal of Civil*
927 *Engineering*, 16(2), 229–238. <https://doi.org/10.1007/s12205-012-0006-1>
- 928 Kosanic, A., Kavcic, I., van Kleunen, M., & Harrison, S. (2019). Climate change and climate change velocity analysis
929 across Germany. *Scientific Reports*, 9(1), 2196. <https://doi.org/10.1038/s41598-019-38720-6>
- 930 Lasslop, G., Reichstein, M., Papale, D., Richardson, A., Arneth, A., Barr, A., Stoy, P., & Wohlfahrt, G. (2010).
931 Separation of net ecosystem exchange into assimilation and respiration using a light response curve approach:
932 Critical issues and global evaluation. *Global Change Biology*, 16(1), 187–208. [https://doi.org/10.1111/j.1365-](https://doi.org/10.1111/j.1365-2486.2009.02041.x)
933 [2486.2009.02041.x](https://doi.org/10.1111/j.1365-2486.2009.02041.x)
- 934 Lausch, A., Heurich, M., & Fahse, L. (2013). Spatio-temporal infestation patterns of *Ips typographus* (L.) in the
935 Bavarian Forest National Park, Germany. *Ecological Indicators*, 31, 73–81.
936 <https://doi.org/10.1016/J.ECOLIND.2012.07.026>
- 937 Law, B. E., Falge, E., Gu, L., Baldocchi, D. D., Bakwin, P., Berbigier, P., Davis, K., Dolman, A. J., Falk, M., Fuentes,
938 J. D., Goldstein, A., Granier, A., Grelle, A., Hollinger, D., Janssens, I. A., Jarvis, P., Jensen, N. O., Katul, G.,
939 Mahli, Y., ... Wofsy, S. (2002). Environmental controls over carbon dioxide and water vapor exchange of
940 terrestrial vegetation. *Agricultural and Forest Meteorology*, 113(1–4), 97–120. [https://doi.org/10.1016/S0168-](https://doi.org/10.1016/S0168-1923(02)00104-1)
941 [1923\(02\)00104-1](https://doi.org/10.1016/S0168-1923(02)00104-1)
- 942 Liu, N. (2017). *Changes in Water and Carbon in Australian Vegetation in Response to Climate Change* [Murdoch
943 University]. <https://researchrepository.murdoch.edu.au/id/eprint/40206/>
- 944 Liu, N. (2021). *R-based Water Supply Stress Index (rWaSSI) model*.
945 <https://sites.google.com/view/rwassi/home?authuser=0>
- 946 Liu, N., Dobbs, G. R., Caldwell, P. V., Miniati, C. F., Bolstad, P. V., Nelson, S., & Sun, G. (2020). *Quantifying the*
947 *role of State and private forest lands in providing surface drinking water supply for the Southern United States*.
948 <https://doi.org/10.2737/SRS-GTR-248>
- 949 Liu, N., SUN, P.-S., Liu, S.-R., & Sun, G. (2013). Determination of spatial scale of response unit for WASSI-C eco-
950 hydrological model—a case study on the upper Zaganuo River watershed of China. *Chinese Journal of Plant*
951 *Ecology*. <https://doi.org/10.3724/SP.J.1258.2013.00000>

- 952 Liu, Z., Shao, Q., & Liu, J. (2015). The performances of MODIS-GPP and -ET products in China and their sensitivity
953 to input data (FPAR/LAI). *Remote Sensing*, 7(1), 135–152. <https://doi.org/10.3390/rs70100135>
- 954 Margulis, S. A., Wood, E. F., & Troch, P. A. (2006). The Terrestrial Water Cycle: Modeling and Data Assimilation
955 across Catchment Scales. *Journal of Hydrometeorology*, 7(3), 309–311. <https://doi.org/10.1175/JHM999.1>
- 956 McCabe, G. J., & Wolock, D. M. (1999). GENERAL-CIRCULATION-MODEL SIMULATIONS OF FUTURE
957 SNOWPACK IN THE WESTERN UNITED STATES1. *JAWRA Journal of the American Water Resources
958 Association*, 35(6), 1473–1484. <https://doi.org/10.1111/J.1752-1688.1999.TB04231.X>
- 959 McNulty, S., Cohen, E., Sun, G., & Caldwell, P. (2016). HYDROLOGIC MODELING FOR WATER RESOURCE
960 ASSESSMENT IN A DEVELOPING COUNTRY: THE RWANDA CASE STUDY. *USDA FOREST
961 SERVICE*. <https://www.fs.usda.gov/treesearch/pubs/53039>
- 962 Morales, P., Sykes, M. T., Prentice, I. C., Smith, P., Smith, B., Bugmann, H., Zierl, B., Friedlingstein, P., Viovy, N.,
963 Sabaté, S., Sánchez, A., Pla, E., Gracia, C. A., Sitch, S., Arneth, A., & Ogee, J. (2005). Comparing and
964 evaluating process-based ecosystem model predictions of carbon and water fluxes in major European forest
965 biomes. *Global Change Biology*, 11(12), 2211–2233. <https://doi.org/10.1111/J.1365-2486.2005.01036.X>
- 966 Pandey, B., & Ghosh, A. (2023). Urban ecosystem services and climate change: a dynamic interplay. *Frontiers in
967 Sustainable Cities*, 5. <https://doi.org/10.3389/frsc.2023.1281430>
- 968 Pastorello, G., Trotta, C., Canfora, E., Chu, H., Christianson, D., Cheah, Y. W., Poindexter, C., Chen, J., Elbashandy,
969 A., Humphrey, M., Isaac, P., Polidori, D., Ribeca, A., van Ingen, C., Zhang, L., Amiro, B., Ammann, C., Arain,
970 M. A., Ardö, J., ... Papale, D. (2020). The FLUXNET2015 dataset and the ONEFlux processing pipeline for
971 eddy covariance data. *Scientific Data*, 7(1), 225. <https://doi.org/10.1038/s41597-020-0534-3>
- 972 Potter, C., & Pass, S. (2024). Changes in the net primary production of ecosystems across Western Europe from 2015
973 to 2022 in response to historic drought events. *Carbon Balance and Management*, 19(1), 32.
974 <https://doi.org/10.1186/s13021-024-00279-9>
- 975 Prescher, A.-K., Grünwald, T., & Bernhofer, C. (2010). Land use regulates carbon budgets in eastern Germany: From
976 NEE to NBP. *Agricultural and Forest Meteorology*, 150(7–8), 1016–1025.
977 <https://doi.org/10.1016/j.agrformet.2010.03.008>
- 978 Pyarali, K. (2024a). *Germany Watershed Delineation*. Figshare.
979 <https://doi.org/https://doi.org/10.6084/m9.figshare.25053599.v1>
- 980 Pyarali, K. (2024b). *WaSSI Model Output*. Figshare. <https://doi.org/https://doi.org/10.6084/m9.figshare.25053641.v1>
- 981 Running, S. W., Mu, Q., Zhao, M., & Moreno, A. (2019a). *User's Guide Daily GPP and Annual NPP
982 (MOD17A2H/A3H) and Year-end Gap-Filled (MOD17A2HGF/A3HGF) Products*.
983 <https://lpdaac.usgs.gov/products/mod17a2hgf006/>
- 984 Running, S. W., Mu, Q., Zhao, M., & Moreno, A. (2019b). *User's Guide MODIS Global Terrestrial
985 Evapotranspiration (ET) Product NASA Earth Observing System MODIS Land Algorithm (For Collection 6)*.
986 <https://doi.org/10.5067/MODIS/MOD16A2GF.006>
- 987 Salerno, F., Gaetano, V., & Gianni, T. (2018). Urbanization and climate change impacts on surface water quality:
988 Enhancing the resilience by reducing impervious surfaces. *Water Research*, 144, 491–502.
989 <https://doi.org/10.1016/j.watres.2018.07.058>
- 990 Schröter, D., Zebisch, M., & Grothmann, T. (2005). *Climate Change in Germany-Vulnerability and Adaptation of
991 Climate-Sensitive Sectors*.
992 [https://www.researchgate.net/publication/232071870_Climate_Change_in_Germany-
993 Vulnerability_and_Adaptation_of_Climate-Sensitive_Sectors](https://www.researchgate.net/publication/232071870_Climate_Change_in_Germany-Vulnerability_and_Adaptation_of_Climate-Sensitive_Sectors)

Formatted: Portuguese (Portugal)

Formatted: Italian (Italy)

Formatted: Italian (Italy)

- 994 Schumacher, E. (2022, January 10). *Natural disasters cost \$280 billion in 2021: German insurance firm* | News | DW
995 | 10.01.2022. [https://www.dw.com/en/natural-disasters-cost-280-billion-in-2021-german-insurance-firm/a-](https://www.dw.com/en/natural-disasters-cost-280-billion-in-2021-german-insurance-firm/a-60378575)
996 60378575
- 997 Smets, B., Swinnen, E., & Van Hoolst, R. (2019). Product User Manual: Dry Matter Productivity and Gross Dry
998 Matter Productivity. Version 2. Collection 1km. In *Copernicus Global Land Services*.
999 <https://land.copernicus.eu/global/products/dmp>
- 1000 Smith, N. E., Kooijmans, L. M. J., Koren, G., Van Schaik, E., Van Der Woude, A. M., Wanders, N., Ramonet, M.,
1001 Xueref-Remy, I., Siebicke, L., Manca, G., Brümmner, C., Baker, I. T., Haynes, K. D., Luijckx, I. T., & Peters, W.
1002 (2020). Spring enhancement and summer reduction in carbon uptake during the 2018 drought in northwestern
1003 Europe. *Philosophical Transactions of the Royal Society B*, 375(1810).
1004 <https://doi.org/10.1098/RSTB.2019.0509>
- 1005 Sun, G., Caldwell, P., Noormets, A., McNulty, S. G., Cohen, E., Myers, J. M., Domec, J.-C., Treasure, E., Mu, Q.,
1006 Xiao, J., John, R., & Chen, J. (2011). Upscaling key ecosystem functions across the conterminous United States
1007 by a water-centric ecosystem model. *Journal of Geophysical Research: Biogeosciences*, 116(G3).
1008 <https://doi.org/10.1029/2010JG001573>
- 1009 Sun, G., Wei, X., Hao, L., Sanchis, M. G., Hou, Y., Yousefpour, R., Tang, R., & Zhang, Z. (2023). Forest hydrology
1010 modeling tools for watershed management: A review. *Forest Ecology and Management*, 530(4), 120755-
1011 <https://doi.org/10.1016/J.FORECO.2022.120755>
- 1012 Sun, S., Sun, G., Caldwell, P., McNulty, S. G., Cohen, E., Xiao, J., & Zhang, Y. (2015). Drought impacts on ecosystem
1013 functions of the U.S. National Forests and Grasslands: Part I evaluation of a water and carbon balance model.
1014 *Forest Ecology and Management*, 353, 260–268. <https://doi.org/10.1016/j.foreco.2015.03.054>
- 1015 Thompson, R. L., Broquet, G., Gerbig, C., Koch, T., Lang, M., Monteil, G., Munassar, S., Nickless, A., Scholze, M.,
1016 Ramonet, M., Karstens, U., Van Schaik, E., Wu, Z., & Rödenbeck, C. (2020). Changes in net ecosystem
1017 exchange over Europe during the 2018 drought based on atmospheric observations. *Philosophical Transactions*
1018 *of the Royal Society B*, 375(1810). <https://doi.org/10.1098/RSTB.2019.0512>
- 1019 Trambauer, P., Dutra, E., Maskey, S., Werner, M., Pappenberger, F., Van Beek, L. P. H., & Uhlenbrook, S. (2014).
1020 Comparison of different evaporation estimates over the African continent. *Hydrology and Earth System*
1021 *Sciences*, 18(1), 193–212. <https://doi.org/10.5194/hess-18-193-2014>
- 1022 Turner, D. P., Ritts, W. D., Cohen, W. B., Gower, S. T., Running, S. W., Zhao, M., Costa, M. H., Kirschbaum, A. A.,
1023 Ham, J. M., Saleska, S. R., & Ahl, D. E. (2006). Evaluation of MODIS NPP and GPP products across multiple
1024 biomes. *Remote Sensing of Environment*, 102(3–4), 282–292. <https://doi.org/10.1016/j.rse.2006.02.017>
- 1025 Ungaro, F., Schwartz, C., & Piorr, A. (2021). Ecosystem services indicators dataset for the utilized agricultural area
1026 of the Märkisch-Oderland District-Brandenburg, Germany. *Data in Brief*, 34, 106645.
1027 <https://doi.org/10.1016/j.dib.2020.106645>
- 1028 Velpuri, N. M., Senay, G. B., Singh, R. K., Bohms, S., & Verdin, J. P. (2013). A comprehensive evaluation of two
1029 MODIS evapotranspiration products over the conterminous United States: Using point and gridded FLUXNET
1030 and water balance ET. *Remote Sensing of Environment*, 139, 35–49. <https://doi.org/10.1016/j.rse.2013.07.013>
- 1031 Verger, A., Descals, A., Benhadj, I., & Claes, P. (2018). *Product User Guide and Specification: CDR VGT-based LAI*
1032 *and fAPAR v1.0*. [http://datastore.copernicus-climate.eu/c3s/published-forms/c3sprod/satellite-soil-](http://datastore.copernicus-climate.eu/c3s/published-forms/c3sprod/satellite-soil-moisture/product-user-guide-v2.3.pdf)
1033 [moisture/product-user-guide-v2.3.pdf](http://datastore.copernicus-climate.eu/c3s/published-forms/c3sprod/satellite-soil-moisture/product-user-guide-v2.3.pdf)
- 1034 Verma, M., Friedl, M. A., Richardson, A. D., Kiely, G., Cescatti, A., Law, B. E., Wohlfahrt, G., Gielen, B., Rounsard,
1035 O., Moors, E. J., Toscano, P., Vaccari, F. P., Gianelle, D., Bohrer, G., Varlagin, A., Buchmann, N., Van Gorsel,
1036 E., Montagnani, L., & Propastin, P. (2014). Remote sensing of annual terrestrial gross primary productivity from

1037 MODIS: An assessment using the FLUXNET la Thuile data set. *Biogeosciences*, 11(8), 2185–2200.
1038 <https://doi.org/10.5194/bg-11-2185-2014>

Formatted: French (France)

1039 Wang, L., Zhu, H., Lin, A., Zou, L., Qin, W., & Du, Q. (2017). Evaluation of the latest MODIS GPP products across
1040 multiple biomes using global eddy covariance flux data. *Remote Sensing*, 9(5).
1041 <https://doi.org/10.3390/rs9050418>

1042 Williams, I. N., Torn, M. S., Riley, W. J., & Wehner, M. F. (2014). Impacts of climate extremes on gross primary
1043 production under global warming. *Environmental Research Letters*, 9(9), 094011. <https://doi.org/10.1088/1748-9326/9/9/094011>

1045 Wu, S., Tetzlaff, D., Goldammer, T., & Soulsby, C. (2021). Hydroclimatic variability and riparian wetland
1046 restoration control the hydrology and nutrient fluxes in a lowland agricultural catchment. *Journal of Hydrology*,
1047 603, 126904. <https://doi.org/10.1016/j.jhydrol.2021.126904>

1048 Zeng, Z., Piao, S., Li, L. Z. X., Wang, T., Ciais, P., Lian, X., Yang, Y., Mao, J., Shi, X., & Myneni, R. B. (2018).
1049 Impact of Earth Greening on the Terrestrial Water Cycle. *Journal of Climate*, 31(7), 2633–2650.
1050 <https://doi.org/10.1175/JCLI-D-17-0236.1>

1051 Zhang, J., Zhang, Y., Sun, G., Song, C., Li, J., Hao, L., & Liu, N. (2022). Climate Variability Masked Greening Effects
1052 on Water Yield in the Yangtze River Basin During 2001–2018. *Water Resources Research*, 58(1),
1053 e2021WR030382. <https://doi.org/10.1029/2021WR030382>

Formatted: Italian (Italy)

1054 Zhang, L., Cheng, L., Chiew, F., & Fu, B. (2018). Understanding the impacts of climate and landuse change on water
1055 yield. *Current Opinion in Environmental Sustainability*, 33, 167–174.
1056 <https://doi.org/10.1016/J.COSUST.2018.04.017>

1057 Zhang, Y., Song, C., Sun, G., Band, L. E., McNulty, S., Noormets, A., Zhang, Q., & Zhang, Z. (2016). Development
1058 of a coupled carbon and water model for estimating global gross primary productivity and evapotranspiration
1059 based on eddy flux and remote sensing data. *Agricultural and Forest Meteorology*, 223, 116–131.
1060 <https://doi.org/10.1016/J.AGRFORMET.2016.04.003>

1061 Zhang, Y., Zhang, Z., Reed, S., & Koren, V. (2011). An enhanced and automated approach for deriving a priori SAC-
1062 SMA parameters from the soil survey geographic database. *Computers & Geosciences*, 37(2), 219–231.
1063 <https://doi.org/10.1016/J.CAGEO.2010.05.016>

1064 Zhu, X., Pei, Y., Zheng, Z., Dong, J., Zhang, Y., Wang, J., Chen, L., Doughty, R. B., Zhang, G., & Xiao, X. (2018).
1065 Underestimates of grassland gross primary production in MODIS standard products. *Remote Sensing*, 10(11).
1066 <https://doi.org/10.3390/rs10111771>

1067 Zimmermann, S., & Hoffmann, K. (2020). Evaluating the capabilities of Sentinel-2 data for large-area detection of
1068 bark beetle infestation in the Central German Uplands. <https://doi.org/10.1117/1.JRS.14.024515>, 14(2),
1069 024515. <https://doi.org/10.1117/1.JRS.14.024515>

1070 Zink, M., Kumar, R., Cuntz, M., & Samaniego, L. (2016). A High-Resolution Dataset of Water Fluxes and States for
1071 Germany Accounting for Parametric Uncertainty. *Hydrology and Earth System Sciences Discussions*,
1072 (September), 1–29. <https://doi.org/10.5194/hess-2016-443>

1073

1074

1075

1076